E. coli-ΦX174 genotype to phenotype map reveals flexibility and diversity in LPS structures

Jordan Romeyer Dherbey, Lavisha Parab, Jenna Gallie and Frederic Bertels

Max Planck Institute for Evolutionary Biology, Plön, Germany

Corresponding authors:
Jordan Romeyer Dherbey (ORCID 0000-0002-6125-1722) and Frederic Bertels (ORCID 0000-0001-6222-4139

Email addresses: dherbey@evolbio.mpg.de, bertels@evolbio.mpg.de

Abstract

Extensive efforts have been made to understand the phenotypic diversity of lipopolysaccharide (LPS) structures through deletion and complementation experiments. However, this approach likely underestimates the available phenotypic diversity. To better explore LPS diversity, we generate LPS mutants in *Escherichia coli* C by selecting for resistance to ΦX174, a bacteriophage that relies solely on binding to core LPS to infect its host. An analysis of 31 *E. coli* C mutants that are resistant to ΦX174 reveals that each mutant carries at least one mutation in genes linked to core LPS biosynthesis or assembly. Based on which genes are mutated, we predict the core LPS structures of each bacterial mutant, and test our predictions by evolving phages to recognize each evolved LPS structure. We find that phages that evolved to infect the same predicted LPS structure were not always able to cross-infect each other's host, suggesting that core LPS structure diversity is higher than predicted. Similarly, phage genotype-phenotype maps can be constructed using the bacterial LPS mutant classes. For example, we demonstrate that a combination of two phage mutations leads to loss of the ability to infect wildtype *E. coli* C. Our results show that phages are a useful tool to study LPS structures, and conversely that the study of LPS structures helps to understand phage evolution and biology.

Keywords: LPS, Overcoming host resistance, Genotype-phenotype maps, Experimental evolution, ΦX174, *E. coli* C.

33 **Introduction**

34

35 Multidrug resistant bacterial infections are one of the most pressing issues in medicine a situation that
36 is only expected to worsen in the coming decades[1–3]. An alternative to treating bacterial infections with
37 antibiotics is phage therapy. Major research efforts are being conducted to develop efficient therapies[4–
38 6]. An efficient therapy should be able to eliminate a pathogen without selecting for resistance to the
39 phage being used to treat that pathogen. Phage resistance can often evolve by modifying the cell
40 envelop to avoid phage adsorption. The outer membrane of all Gram-negative bacteria is covered in
41 lipopolysaccharides (LPSs), which is consequently the first contact point between a bacterium and its
42 environment[7]. LPS structure determines whether a bacterium will be recognized by the immune
43 system, whether it is susceptible to antibiotics, determines the efficiency of nutrient uptake and,
44 importantly, determines susceptibility to phage infection[8–10]. Hence, LPS structure is an important
45 factor determining the success of phage therapy.

46

47 The functions of almost all genes involved in synthesizing and assembling bacterial lipopolysaccharide
48 (LPS) have been eluciated[11–15]. Most *Escherichia coli* strains produce LPS molecules composed of three
49 parts: the lipid A, the core oligosaccharide (OS; itself consisting of a conserved inner core and an outer
50 core), and the O-antigen chain. Such tripartite LPS molecules are termed "smooth"[12]. Some *E. coli*
51 strains produce LPS molecules that lack one or more components. LPS molecules lacking the O-
52 antigen are classified as "rough", molecules lacking the O-antigen and the OS outer core, as "deep
53 rough"[15,16,11,17–19]. These modifications in LPS structure can lead to a plethora of phenotypic effects,
54 including (i) destabilization of the outer membrane[12], (ii) changes in the expression of some outer
55 membrane proteins and (iii) modification of intracellular turgor pressure[20], (iv) increased susceptibility
56 to hydrophobic compounds such as antimicrobial peptides, antibiotics, and bacteriocins[15,16,11,17–19], (v)
57 altered interactions with the host immune system[21,12], and (vi) changes in resistance to phages[9,22–24].

58

59 Phage ΦX174 is a small (~320 Å), tailless coliphage from the Microvirus family. It carries a circular,
60 single-stranded DNA genome of only 5386 bp that encodes 11 genes[25,26]. To enter a host cell, ΦX174
61 relies solely on attaching to the core OS by one of its spike proteins before migrating and irreversibly
62 adsorbing to the host's cell surface via its capsid[27–29]. ΦX174 does it with a high degree of specificity:
63 in one study, among 783 different *E. coli* isolates, only six (0.8 %) could be infected by wildtype

ΦX174[30]. In the laboratory ΦX174 infects - and hence is usually grown on - *E. coli* C, which produces rough type (*i.e.*, lacking in O-antigen) LPS molecules[31–34] (**Figs. 1 and S1**).

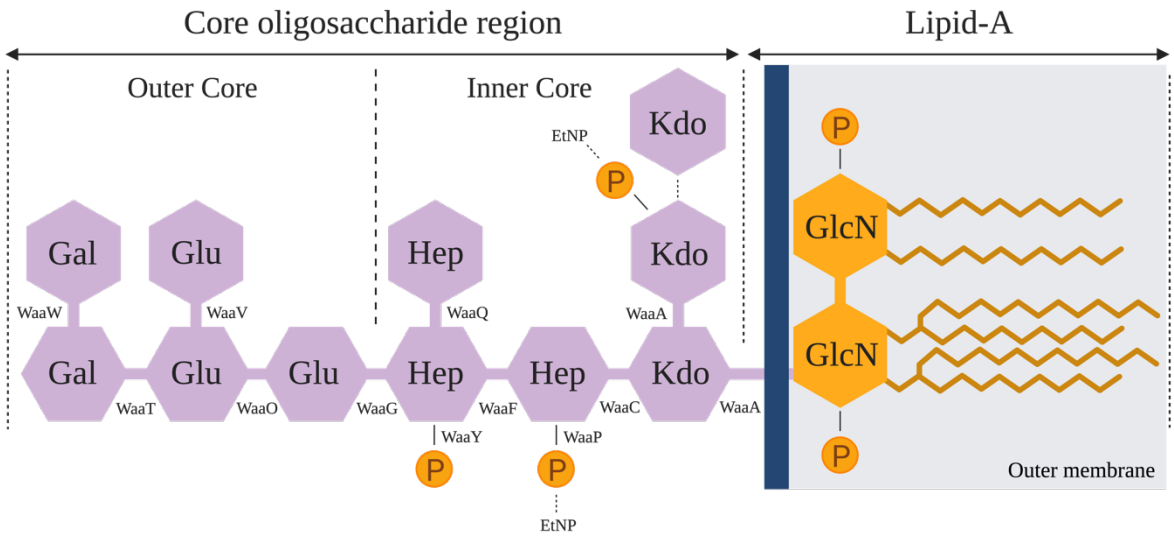

Fig. 1. Structure of *E. coli* C's rough type LPS. The rough type LPS of *E. coli* C is composed of two parts: lipid A (composed of an acetylated and 1,4'-diphosporylated β(1→6)-linked glucosamine (GlcN) disaccharide), and the core oligosaccharide[12]. The core oligosaccharide is subdivided into a structurally conserved inner core and an outer core. The dashed lines show non-stochiometric substitutions of phosphate (P), ethanolamine (EtNP), and 3-deoxy-D-*manno*-octulosonic acid (Kdo) residues on the LPS[35]. Details of the LPS assembly process are provided in **Fig. S1**.

Here, we explore the evolutionary potential of *E. coli* C to become resistant to infection by ΦX174 and, conversely, the potential of ΦX174 mutants to infect phage-resistant *E. coli* C hosts with modified LPS structures. We first generate a set of 31 *E. coli* C mutants that are resistant to infection by ΦX174 wildtype and determine that each mutant carries at least one mutation affecting LPS biosynthesis.

The currently accepted model for predicting LPS structure posits that the presence or absence of each LPS gene leads to a single LPS phenotype. Based on the position of each mutation, the one-gene-one-phenotype model allows us to predict the LPS structure of each of our LPS mutants. Our 31 *E. coli* C mutants collectively produce LPS molecules with seven distinct structures. To test the accuracy of these predictions, we evolved and genotypically characterized a set of sixteen ΦX174 genotypes that can, between them, infect all initially resistant 31 *E. coli* C mutants. If the LPS structure predictions are correct then all bacteria predicted to carry the same LPS structure should be susceptible to the

same set of phages. Interestingly, this was not always the case, indicating that the diversity of LPS structures generated by LPS-pathway mutations is much higher than anticipated from previous studies. Bacterial strains with different mutations in the same LPS gene sometimes have strikingly different infection phenotypes. Even the required number of phage mutations to overcome these resistances can differ significantly. A better understanding of the evolution of phage resistance hence requires a better understanding of the biology and evolution of LPS structures.

Results

Diverse LPS structures confer resistance to ΦX174 infection

To study LPS diversity in *E. coli* C, we generated 35 spontaneous phage-resistant strains, and used whole genome re-sequencing to identify the mutation(s) conferring resistance (see **Methods**). Due to a lack of isogeneity or only a partial resistance to wildtype ΦX174, four of these strains (*E. coli* C R1, R3, R15, and R19) were excluded from downstream analyses (see **Text S1**). Of the remaining 31 strains, 27 are predicted to carry a single mutation, three carry two mutations, and one carries three mutations (see **Table S1**). A total of 36 mutations were identified, 32 of which are unique (including 15 nucleotide substitutions, 13 deletions, one duplication, and three IS*4* and IS*5* insertion events). Twenty-four (of 32, or 75%) mutations introduce premature stop codons or lead to frameshifts, and thus are highly likely to disrupt gene function.

Interestingly, two of these mutations are shared by two strains (R27/R31 and R8/R10), and one mutation is shared by three strains (R4/R24/R29). Given that there are almost limitless ways to disrupt gene function, this high degree of parallelism is initially surprising. We note that the repetition of these mutations is unlikely to result from their positive selection. That is, phage-resistant *E. coli* C mutants of both low and high fitness are expected to have an equal chance of appearing on our agar plates (as long as they can form visible colonies)[36]. Presumably, the observed parallelism is instead due to elevated mutation rates at particular genomic positions[37]. The fact that two of three parallel mutations occur in homopolymeric tracts supports this hypothesis[38].

Mutations in genes encoding the LPS machinery are expected to lead to changes in LPS structure, and in some cases, LPS type[17,18,39]. Logical predictions of mutant LPS structures can be made according to the "LEGO® block" principle; if an enzyme that synthesizes a particular LPS component is absent or non-functional, then that LPS component cannot be synthesized. In addition, LPS components

118 assembled downstream of the missing component are also absent from the final LPS structure. Under
119 the assumption that each mutation in an LPS gene leads to a complete lack of function, this LEGO®
120 block principle was used to predict the LPS structure and type of each of the 31 *E. coli* C phage-
121 resistant mutants (**Figs. 2**, **S1**, **S2 and Table S1**). A total of seven emergent LPS structures were
122 forecast from our set of mutants (**Fig. 2**). Compared with the *E. coli* C wildtype LPS, three of these
123 seven LPS structures carry alterations in the outer-core OS, and hence are predicted to be rough type
124 (as is wildtype *E. coli* C; ten mutants). The remaining four LPS structures differ from wildtype LPS in
125 both the inner- and outer-core OS, and are presumed to be of the deep rough type (twenty mutants)
126 (see **Table S1**). The LPS structure and type of the remaining mutant (*E. coli* C R25) was not predicted,
127 because the effect of the phage-resistance mutation on LPS biosynthesis remains unclear; specifically,
128 R25 carries a nonsense mutation in *rfaH*. The *rfaH* gene encodes a transcriptional antiterminator that
129 regulates the *waa* operon[14,40], meaning that any number of LPS biosynthetic genes could potentially be
130 affected by this mutation.
131

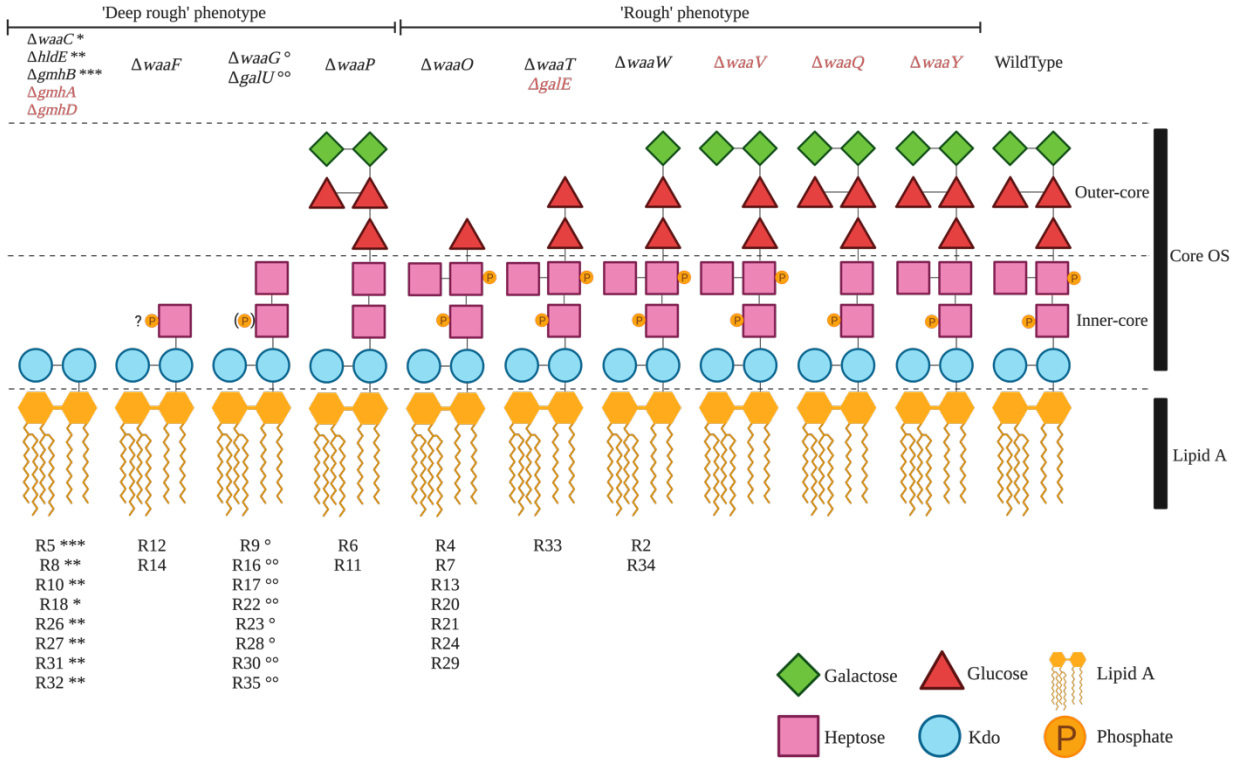

132

133 **Fig. 2. Predicted LPS structures of 30 ΦX174-resistant *E. coli* C strains.** Predicted LPS structures fall into
134 two groups depending on their degree of truncation and/or loss of phosphate groups: the "deep rough"
135 phenotype with a completely truncated outer core or a loss of phosphate groups (twenty *E. coli* C mutants), and

136 the "rough" phenotype with smaller LPS truncations located in the outer core (ten *E. coli* C mutants). The LPS
137 phenotype of the final *E. coli* C mutant (R25) could not be predicted (see text). The products of genes in red
138 are also involved in LPS biosynthesis and, although no mutations were identified in these genes during this
139 study, are also potential targets for phage-resistance. Details on the functions of *gmhA*, *gmhB*, *gmhD*, *hldE*, *galU*,
140 and *galE* are provided in **Fig. S2**. "?P": No information was found on the phosphorylation of Hep(I) in the
141 absence of *waaF*; (P): only 40% of the hexose phosphorylation was observed[39]; R#: the number gave to each
142 *E. coli* C resistant strain; "*, **, ***, °, °°": identical symbols indicate that different genes are inactivated but are
143 expected to lead to the same LPS core structure.
144
145 The LPS structure predictions above can be tested by evolving wildtype ΦX174 to specifically infect
146 *E. coli* C cells with modified LPS structures. That is, a phage that can infect a given modified LPS
147 structure is expected to be able to infect all bacterial strains displaying this LPS type, regardless of the
148 underlying mutations. Alternatively, the inability of mutant phages to cross-infect bacterial strains of
149 the same predicted LPS structural class (but via different mutations) would indicate that these
150 mutations actually lead to distinct LPS structures.
151
152 **ΦX174 evolves to overcome host resistance, a process that can be accelerated by host diversity**
153 Phages that can infect resistant *E. coli* C mutants were evolved by serially transferring wildtype ΦX174
154 on each of the 31 resistant *E. coli* C strains (**Fig. 3A and Methods**). To reduce the complexity of the
155 experiment, bacterial cultures were not allowed to co-evolve. Instead, phages were inoculated into
156 fresh, exponentially growing host cultures at each transfer. The experiment gave rise to twelve evolved
157 phages that were collectively able to infect 21 (of the 31) initially resistant *E. coli* C strains (these display
158 the "easy" resistant phenotype; see **Table S2**). However, even after 21 transfers, ten (of 31) resistant
159 *E. coli* C strains remained uninfected (the "hard" resistant phenotype; see **Table S2**). To increase the
160 chances of evolving phages capable of infecting these strains, two further evolution experiments were
161 designed (**Figs. 3B and 3C**). In both of these experiments, phage diversity was increased by
162 combining all evolved phage strains into a phage cocktail[41,42]. Phage diversity was maintained from
163 one transfer to another by adding all corresponding resistant strains to the host culture (see **Methods**).
164 The phage cocktail was serially transferred once per day in the second evolution experiment, while
165 four transfers per day were performed in the third evolution experiment. At the end of the third
166 evolution experiment, while six *E. coli* C resistant strains remained uninfected by their own phage, all
167 resistant strains could be cross-infected by at least one evolved of the phage mutant. Our method of

168 isolating re-infecting phage is simple and effective, and allowed the successful retrieval of phages that
169 can target any of the 31 resistant phenotypes.
170
171 Increasing both phage and host diversities in the second and third evolution experiments accelerated
172 the adaptation of ΦX174. This result seemingly contradicts recent research by Sant *et al.*, which
173 elegantly shows that higher host diversity decreases the rate at which phages evolve[43]. By adapting
174 phage ΦJB01 (a phage that likely uses the LPS to infect its *E. coli* host[43]) to a set of different *E. coli*
175 strains, the authors demonstrate that adaptation to resistant (non-permissive) strains is faster in
176 evolution experiments where ΦJB01 is exposed to only one permissive and one non-permissive host,
177 than when two non-permissive and one permissive strain are used. Similar to the two-strains
178 experiment of Sant *et al.*[43], in our first evolution experiment, we evolved phage ΦX174 in the presence
179 of one permissive and one non-permissive *E. coli* C strain. While the experiment quickly gave rise to
180 phages able to infect most of the non-permissive strains (**Fig. 4A**), some phage-resistant hosts could
181 only be infected when both host and phage diversities were increased (**Fig. 4B-C**).
182

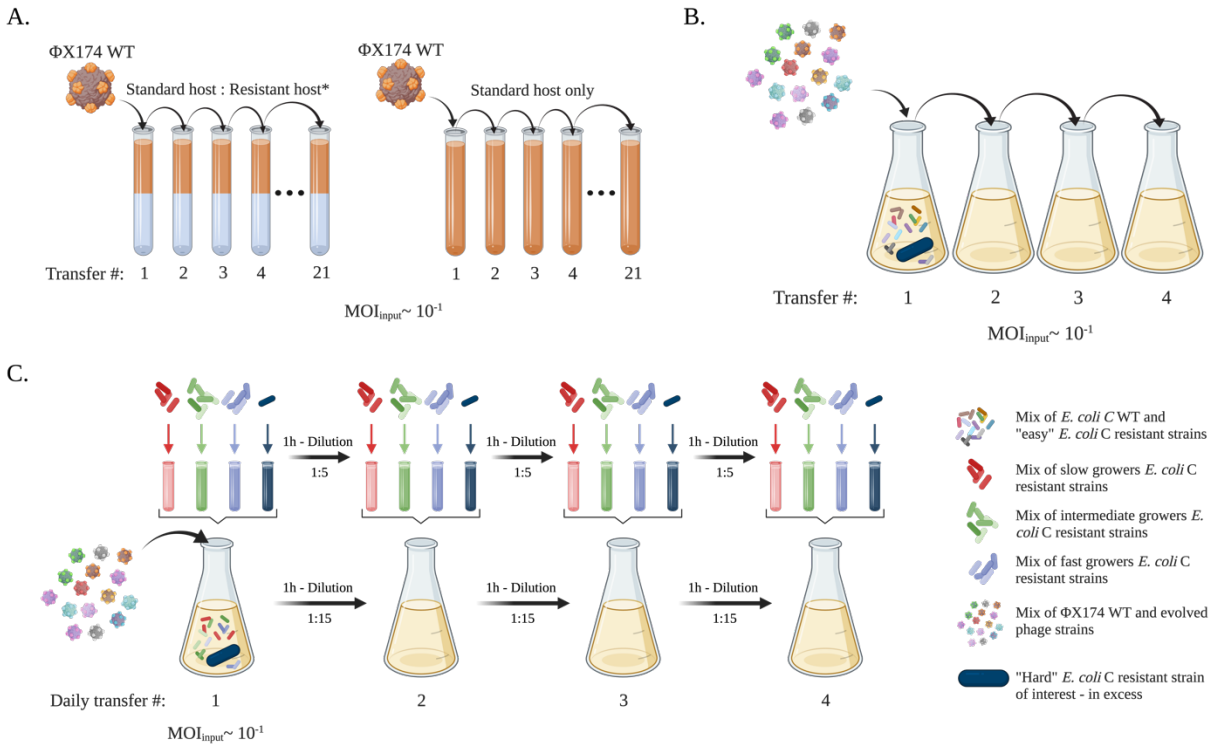

183
184 **Fig. 3. Three phage evolution experiments used to overcome *E. coli* C resistance to wildtype ΦX174.**
185 **A.** First evolution experiment (standard): 31 independent lineages, each founded by ΦX174 wildtype, were
186 serially transferred for up to 21 transfers. Phage were grown on non-evolving (i.e., freshly prepared at each

187 transfer) host cultures containing a mixture of *E. coli* C wildtype and one of the 31 initially resistant strains (see
188 **Table S1**). Phages capable of infecting the initially resistant host strain were isolated from 12 lineages. Three
189 control lineages, where ΦX174 was cultured on only *E. coli* C wildtype, were included. **B.** Second evolution
190 experiment (increased diversity). Four independent lineages were founded by a cocktail of ΦX174 wildtype and
191 the 14 evolved ΦX174 strains (panel A – two evolved phages were removed from mutational analysis, see **Text**
192 **S1**). Each lineage was transferred daily for up to four days, on non-evolving host cultures containing (i) *E. coli*
193 C wildtype, (ii) the 14 host strains for which resistance had been overcome (permissive hosts), and (iii) an excess
194 of the still-resistant strain of interest (non-permissive host). Phages capable of infecting the resistant strain of
195 interest were isolated from two lineages. **C.** Third evolution experiment (increased diversity and generations).
196 Two lineages were founded by the same cocktail used for the second evolution experiment (panel B). However,
197 each lineage was transferred four times daily for up to four days (i.e., a maximum of 16 transfers), on non-
198 evolving host cultures containing (i) *E. coli* C wildtype, (ii) the 14 strains for which resistance had been overcome
199 (permissive hosts), and (iii) the still-resistant strain of interest (non-permissive host). Notably, all transfers
200 completed on the same day involved transferring both phage and bacteria; on every fourth transfer,
201 supernatants were collected and only phage transferred. Phages capable of infecting the resistant strain of
202 interest were isolated from the two lineages. Details of the evolved phages are presented in **Table S2**, and
203 further methodological details are provided in **Methods**.
204

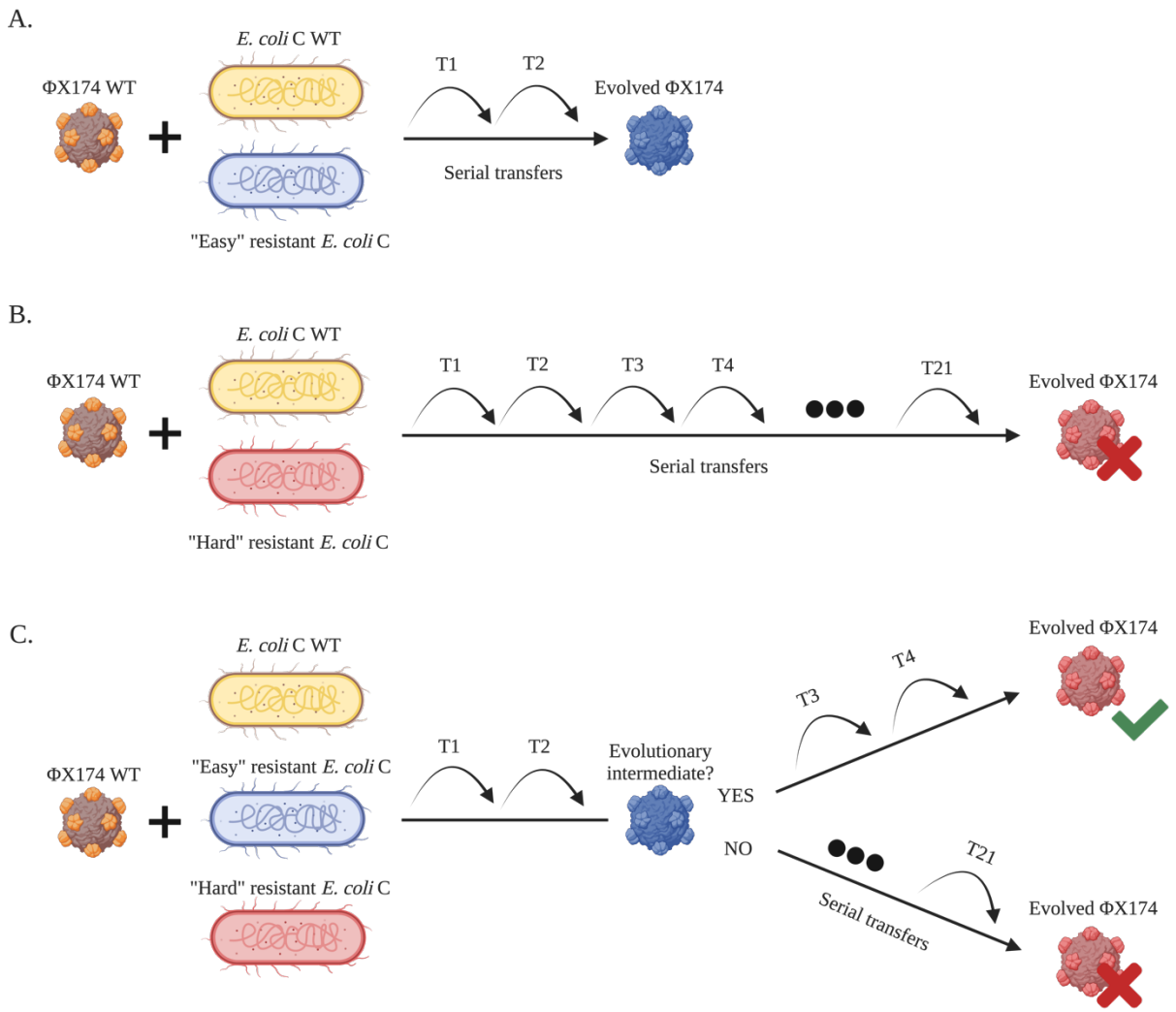

Fig. 4. Increased host diversity facilitates viral adaptation. A. ΦX174 wildtype evolves on *E. coli* C wildtype and an "easy" *E. coli* C resistant strain. Adaptation to the resistant mutant is fast, and requires few transfers. **B.** ΦX174 wildtype evolves on *E. coli* C wildtype and a hard *E. coli* C resistant strain that it failed to infect within 21 standard serial transfers. Infecting this resistant strain may be difficult and take a long time. **C.** ΦX174 wildtype evolves in a three-host mix containing *E. coli* C wildtype and two *E. coli* C resistant strains: one easy and one hard. Phage adapts quickly to the easy resistant phenotype. If the infection of the easy resistant strain leads to the production of an evolutionary intermediate phage, then the hard phenotype can be infected after a few more transfers. If no evolutionary intermediate phage is produced, then no phage evolves to infect the hard resistant *E. coli* C strain.

217 To identify the mutation(s) responsible for the re-infection of the resistance mutants, we performed
218 whole genome re-sequencing on the 16 evolved phages (isogenic isolates) that successfully overcame
219 the corresponding resistance in one of the three evolution experiments (see **Methods**). We found
220 mutations in *F* and/or *H* genes in all 16 (**Table S2**) and discuss their molecular details in depth in the
221 subsequent section. Notably, all hard resistant *E. coli* C strains - those whose resistance was overcome
222 in the second and/or third evolution experiments - are only infected by phage carrying four mutations
223 (see **Tables S1 & S2**). The evolutionary emergence of a multi-mutation phage is expected to require
224 a large number of transfers in a two-strain evolution experiment (**Fig. 4B**). However, this process is
225 significantly accelerated by propagating a diverse mixture of phages that can overcome easy resistance,
226 some of which may act as evolutionary intermediates (i.e., carry a subset of mutations required to
227 overcome hard resistance). The mutational sets required to overcome hard resistance can subsequently
228 emerge in a single mutational step, either by recombination[44] or by *de novo* mutation (**Fig. 4C**). For
229 example, hard resistant strain *E. coli* C R22 (a *galU* mutant; see **Table S1**) is overcome in the second
230 evolution experiment by ΦX174 R22 T1, a phage that carries four mutations (three in *F*, one in *H*;
231 see **Table S2**). Each of these mutations was present in the phage cocktail used to initiate the
232 evolutionary lineage: ΦX174 R18 T4 (which overcomes the easy resistance of *E. coli* C R18) contains
233 three of the four mutations, and the final mutation is found in ΦX174 R10 T6 (which overcomes the
234 easy resistance in *E. coli* C R10). Thus, adaptation to an easy resistant LPS structure (e.g., that of *E.*
235 *coli* C R18) yields an evolutionary intermediate phage that can more easily evolve to infect a hard
236 resistant LPS structure (e.g., that of *E. coli* C R22).
237
238 While adaptation to re-infect easy resistant host strains can be rapid under low host diversity (as shown
239 in previous studies[43,45]), the results in this section demonstrate that it can be nearly impossible to infect
240 hard *E. coli* C resistant strains in the absence of additional hosts that allow the evolution of
241 intermediate phages.
242
243 **ΦX174 overcomes *E. coli* C resistance by mutations in the F capsid and H minor spike**
244 **proteins**
245 The 16 evolved phages collectively carry 40 mutations, 15 of which are unique (**Fig. 5A and Table**
246 **S2**). All are non-synonymous and occur in either *F* (encoding the viral capsid, with mutations
247 occurring specifically in regions encoding the E-F and H-I loops[46]; the loops are involved in the
248 irreversible adsorption of the capsid to the bacterium's cell surface[29]) or *H* (encoding the minor spike

249 protein involved in viral DNA injection) (**Figs. 5B & C**). Almost all evolved phages (13 of 16, or
250 ~81%) carry multiple (between two and four) mutations (**Fig. 5D**). These results are consistent with
251 previous studies demonstrating that mutations in *F* and *H* are relevant for the adaptation of ΦX174
252 to novel hosts[47–49].
253
254 Parallel evolution was common in our evolved phages, particularly in the control lines and the lineages
255 (populations) that failed to infect their corresponding resistant *E. coli* C strains (see **Table S3**). Of the
256 three controls and 15 resistant lines (the phage infecting R5 was removed from the mutational
257 analyses, see **Text S1**) that remained uninfected by their own phage, a total of 33 mutations were
258 detected, but only ten were unique. All of these mutations are located in the *F* gene, except one in the
259 *A*/*A** genes (at genomic position 4817). The mutation in the *F* gene at genomic position 2280 (causing
260 amino acid change S427L in the F protein) arose in 13 lineages. Among them, nine (69 %) present
261 between one to three additional mutations. High degrees of parallel evolution have also previously
262 been observed in ΦX174 wildtype strains and other viruses[50–54], and is an indicator of either (i) a low
263 number of mutational targets with high fitness gains, or (ii) mutational bias towards certain positions
264 in the genome[37,54].
265
266 We also observed high levels of parallel evolution in the isogenic phage strains that evolved to infect
267 *E. coli* C mutants with the same predicted LPS phenotype (**Figs. 5A and 5B**). Parallelism was especially
268 remarkable among phages infecting the four bacterial strains with the shortest (deep rough
269 heptoseless) predicted LPS structure (see **Fig. 2**). The four phages infecting *E. coli* C R18, R8, R10,
270 and R26 all carry an amino acid substitution at position 154 in the F protein (either Q154K or Q154R).
271 In addition, the two phage strains adapted to the *E. coli* C mutants R8 (*hldE* mutant) and R18 (*waaC*
272 mutant) also carry the mutations Y103H in the F protein and A68T in the H protein. Finally, while *E.*
273 *coli* C R27 and R31 both became resistant via the same amino acid substitution in HldE (G27A), their
274 corresponding phages evolved similarly to re-infect by each acquiring a different mutation that led to
275 the same change at the protein level (G91V in the H protein).
276

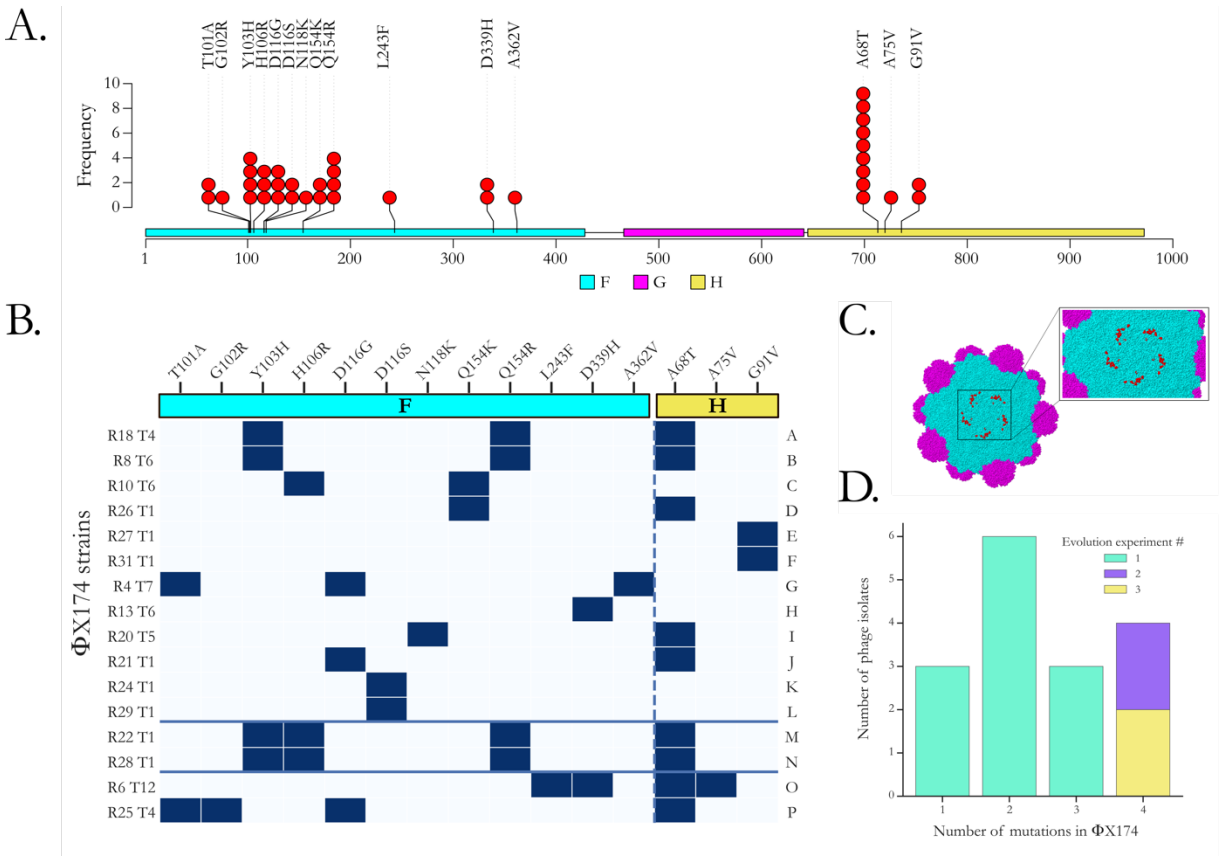

Fig. 5. Adaptation of ΦX174 to resistant strains of *E. coli* C. A. Positions of all predicted amino acid changes in the F and H proteins observed in the 16 evolved ΦX174 strains. **B.** Substitution matrix of all amino acid changes observed in ΦX174. ΦX174 strains are ordered based on the predicted LPS structures they infected during the evolution experiments (A-F: overcame heptoseless *waaC* and *hldE* mutants; G-L: overcame *waaO* mutants; M-N: overcame *galU* and *waaG* mutants; O: overcame *waaP*/*pssA* mutant; P: overcame *rfaH* mutant). The solid blue lines separate the evolved phages according to the evolution experiment from which they were isolated (A-L: first; M-N: second; O-P: third). The x-axis shows amino acid substitutions in the F and H proteins (separated by the dashed line), R# indicates the resistant bacterial strain that the phage evolved on, and T# is the number of transfers required to overcome host resistance. **C.** Location of protein changes on the ΦX174 three-dimensional structure. The F capsid proteins are coloured in cyan and the G major spike proteins are in magenta. Residues affected by the mutations in this study are in red and shown for one F capsid unit only. The G protein spike (above that pictured here) has been removed to improve visualisation. The image was generated using Geneious prime (version 2020.1.2) and Protein Data Bank accession code 2BPA[46]. Changes in the H protein cannot be displayed as they all occur outside of the currently determined crystallographic structure. **D.** Barplot of the number of evolved phage isolates carrying 1, 2, 3, 4 mutations. Most phage isolates – particularly those isolated from the second and third evolution experiments – carry multiple mutations.

295 Parallel evolution was also observed in phages infecting bacteria within several other classes of
296 predicted LPS structure. For example, the evolved phages infecting *galU* mutant *E. coli* C R22 and
297 *waaG* mutant *E. coli* C R28 carry an identical set of four mutations, one in the *H* gene and three in the
298 *F* gene (**Table S2 and Fig. 5**). Another example is the mutation at position 116 in the F protein (either
299 D116G or D116S) that occurred in four different phages all infecting different *waaO* mutants (**Figs.**
300 **5A and 5B**, **Table S2**). Parallel evolution in phages that evolved to infect *E. coli* C strains with the
301 same predicted LPS structure generally support the predicted classes of LPS structure. However,
302 analyses in the following section demonstrate that LPS structure predictions generally underestimate
303 LPS diversity.
304
305 **Evolved phages can be used to discriminate between LPS phenotypes**
306 To determine precisely which of the 31 initially resistant *E. coli* C strains each of the 16 evolved phages
307 can infect (i.e., the infection pattern of each phage), a cross-infection assay was performed (**Fig. S3**).
308 This involved measuring the infectivity of all possible host-phage combinations by two distinct
309 methods: (i) phage spotting on host lawns, and (ii) host spotting on phage lawns. In cases where a
310 mismatch between the two results was observed, standard plaque assays were used as a tie breaker
311 (see **Methods**). If our predictions – which are based on current literature in the field – of seven distinct
312 LPS structures among the 31 initially resistant *E. coli* C strains are accurate (see **Fig. 2 and Table S1**),
313 then all phages that evolved to infect a mutant with a given predicted LPS structure are expected to
314 be capable of cross-infecting all other host strains with the same predicted LPS structure. That is, the
315 infection patterns in **Fig. S3** would be identical for each class (colour) of *E. coli* C mutant. To visually
316 determine whether infection patterns at least cluster according to predicted LPS structure, a
317 hierarchical agglomerative clustering analysis was performed on the infection matrix in **Fig. 6**. Of the
318 six predicted LPS structures that occur in at least two *E. coli* C mutants, three form unbroken clusters
319 with respect to infectivity pattern (cyan, light purple, and dark purple highlighting in **Fig. 6**) and three
320 do not (magenta, yellow, green highlighting). Each group is discussed in more detail below.
321
322 *LPS predictions that cluster by infection pattern.* Firstly, ΦX174 mutants R22 T1 and R28 T1 - isogenic
323 phages that evolved to infect resistant strains with mutations in *galU* (*E. coli* C R22) and *waaG* (*E. coli*
324 C R28) - can cross-infect all eight *E. coli* C mutants predicted to exhibit the same LPS structure (*E. coli*
325 C R9, R16, R17, R22, R23, R28, R30, R35; highlighted in cyan in **Figs. 6 and S4**). Secondly, both *E.*
326 *coli* C *waaW* mutants (R2 and R34; light purple) are cross-infected by the same three evolved phage

327 genotypes (R6 T12, R13 T6, R25 T4). Thirdly, both *E. coli* C *waaF* mutants (R12 and R14; dark purple)
328 are infected by a near-identical set of seven (R12) or six (R14) phages. In each of these cases, phage
329 infectivity patterns appear to be a good indicator of host LPS phenotype (and, to some extent,
330 underlying host genotype).
331

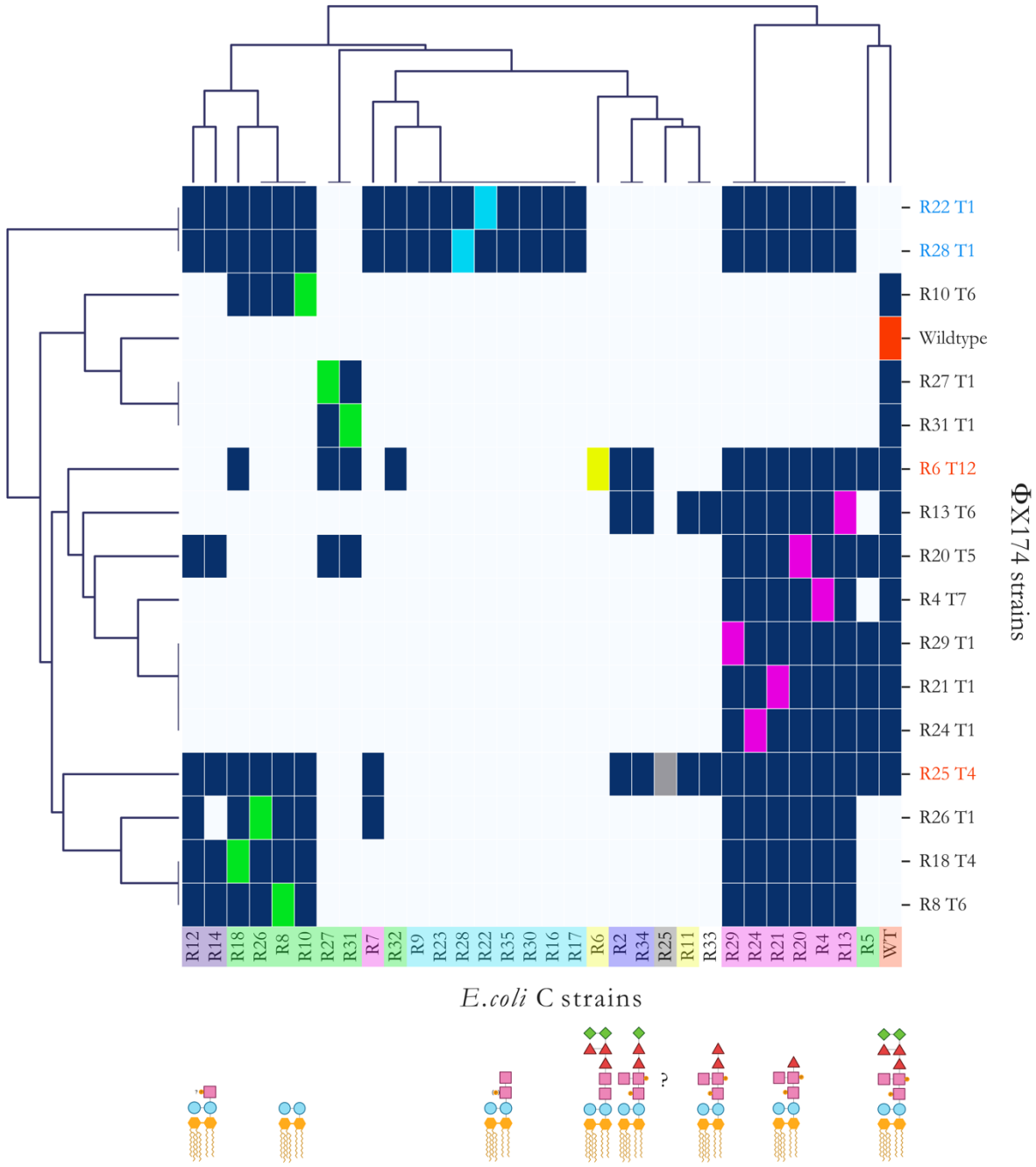

332

333 **Fig. 6. Hierarchical agglomerative clustering analysis of the host ranges of evolved phage.** To
334 unravel structures in the heatmap infection matrix (see **Fig. S3**), we performed a clustering analysis
335 using the default settings of the Seaborn library (version 0.11.2) for Python (version 3.7.4). Briefly,
336 each data point is considered as a cluster. The linkage method computes the distance between them,
337 then repeatedly combines two nearest clusters into larger clusters, until a single cluster is left. *E. coli* C
338 strains are coloured based on their predicted core LPS structure (see **Fig. 2**). Phage names in black
339 were obtained during the first 21 serial transfers (first evolution experiment). Phage strains in blue
340 were obtained in the second evolution experiment (phage cocktail, one transfer per day). Phage strains
341 in red were obtained in the third evolution experiment (phage cocktail, four transfers per day). Dark
342 blue squares=infection, light blue square=no infection, coloured square=control infection by a phage evolved
343 on that host. R# indicates the number of the resistant strain the phage evolved on, and T# is the transfer
344 number where plaques were first observed. "?": core LPS structure of *E. coli* C R25 (*rfaH* mutant) could not be
345 predicted.
346
347 *LPS predictions that do not cluster by infection pattern.* Firstly, the six of the seven *E. coli* C *waaO* mutants
348 (highlighted in magenta in **Figs. 6 and S4**) can be cross-infected by the same set of six phages. The
349 seventh *waaO* mutant (*E. coli* C R7) was the only *waaO* mutant for which the corresponding phage
350 lineage did not evolve to infect the resistant mutant in the first evolution experiment; it can only be
351 infected by the phage infecting R26 and phages that evolved in the second and third evolution
352 experiments (**Fig. 6**). Hence, it is likely that the LPS structure of R7 differs from that of the other
353 *waaO* mutants. The difference could conceivably result from residual (or altered) WaaO function; *E.*
354 *coli* C R7 carries an in-frame deletion of a 6-bp repeat in *waaO*, which alters two WaaO residues, but
355 leaves the remainder of the protein intact (see **Table S1**). While it may be possible that the LPS
356 structure of R7 resembles that of *galU*/*waaG* mutants (**Figs. 2 and S4**), more detailed LPS studies are
357 needed to elucidate the LPS structure of R7.
358
359 Secondly, the infection patterns of the two *waaP* mutants *E. coli* C R6 and R11 (highlighted in yellow
360 in **Figs. 6 and S4**) also do not fit with the LPS structure prediction; R6 is infected by a single phage
361 that evolved directly on host R6 (phage R6 T12 from the third evolution experiment), while R11 is
362 cross-infected by two different phages (phage R13 T6 from the first evolution experiment, and R25
363 T4 from the third). The cluster map analysis indicates that R11 displays an LPS phenotype comparable
364 to the rough LPS phenotype of R33, a *waaT* mutant (**Fig. 6**). *E. coli* C R6 was the last resistant strain

365 to be infected by an evolved phage, and the evolved phage infecting R6 cannot cross-infect R11.
366 Therefore, the location and nature of the mutation in *waaP* strongly impact the LPS structure, possibly
367 by affecting the number of phosphorylated hexoses in the inner core LPS (see **Fig. S1**).
368
369 Thirdly, eight deep rough *E. coli* C mutants are predicted to have the shortest possible LPS structure
370 (**Fig. 2**; green highlighting in **Figs. 6 and S4**). Yet the combination of phages that can infect each of
371 them is remarkably different, with these *E. coli* C strains clustering into four different phenotypic sub-
372 groups (**Fig. 6**). The first sub-group consists of *E. coli* C R8, R10, R18, and R26. Each of these strains
373 can be cross-infected by their corresponding evolved phages regardless of their genotypes (a mixture
374 of *waaC* or *hldE* mutants). However, none of the four evolved phages can cross-infect *E. coli* C R27
375 or R31 (*hldE* mutants). *E. coli* C R27 and R31 constitute the second sub-group, in which both bacteria
376 and their corresponding evolved phages acquired identical genotypes and phenotypes. *E. coli* C R5
377 (*gmhB* mutant) and *E. coli* C R32 (*hldE* mutant) fall into a third and fourth sub-groups. They are the
378 only deep-rough mutants for which the corresponding phage lineages failed to adapt during the first
379 evolution experiment. Only a very narrow but different set of evolved phages can infect them
380 (especially for R32), and none of them belongs to the first or second deep rough LPS phenotypic
381 group.
382
383 The phenotypic differences observed in the four groups are not due to the involvement of *hldE*, *waaC*,
384 and *gmhB*, since a total loss of function in any of these genes always leads to a complete truncation of
385 the inner core LPS (**Fig. S2B**). *E. coli* C R8, R10, R18, and R26 belong to the same phenotypic group
386 despite having either *hldE* or *waaC* mutated, while neither R27, R31, or R32 (*hldE* mutants) belong to
387 this group (**Table S1**, **Fig. 6**). The involvement of the *gmhB* gene in *E. coli* C R5 might be an exception.
388 Previous research demonstrated that the deletion of *gmhB* only caused a partial defect in the synthesis
389 of the LPS core, resulting in the formation of heptoseless and heptose-rich forms[55]. However, the lack
390 of other resistant strains carrying mutations in *gmhB* in our dataset makes it unclear whether any
391 mutation in *gmhB* leads to the same mix of a unique deep rough and the WT phenotypes or if multiple
392 deep rough phenotypes can appear and persist. Nonetheless, the phenotype exhibited by R5 is
393 strikingly close to the one of *E. coli* C WT (**Fig. 6**). Thus, the involvement of these three genes in the
394 production of the deep rough phenotypes cannot explain the vast phenotypic diversity in LPS
395 structures. Instead, the location and type of mutation are more likely to cause the observed LPS
396 structure diversity.

397

398 Our infectivity assay demonstrates that predictions of LPS structure based on mutated gene(s) are not
399 always – or even often - accurate. Mutations are not simple knock-out mutations as previously
400 assumed but can have much more subtle effects on LPS structure. Hence, the "LEGO® block"
401 principle (see section **Diverse LPS structures confer resistance to ΦX174 infection**) is an
402 oversimplified model that does account for all structural alterations and how they can be they can be
403 regulated[14]. Phage infectivity patterns, however, provide a much better indicator of LPS structure and
404 can be used to link bacterial genotypes to their LPS phenotypes.

405

406 **Linking phage genotype to phenotype**

407 Similar to how phages can be used to link bacterial genotypes to LPS phenotypes, we can –
408 theoretically - use evolved bacteria to link phage genotypes to infection phenotypes. While there are
409 not many instances that unequivocally allow us to tie a mutation to a genotype, we can tie the
410 phenotype of infecting *E. coli* C wildtype to a specific phage genotype. Every phage strain that loses
411 the ability to infect the wildtype has a combination of two mutations: A68T in the H protein and
412 Q154K/R in the F protein (**Figs. 5B & 6**). In isolation, A68T confers the ability to infect *waaO*
413 mutants and Q154K/R [R8, R18, R10, R26]-heptoseless mutants. While the two mutations combined
414 allow the phage to infect both heptoseless and *waaO* mutants, the phage loses the ability to infect the
415 *E. coli* C wildtype. Phage R25 is the only phage that can infect all three genotypes: *waaO*, the [R8, R18,
416 R10, R26]-heptoseless mutants, and *E. coli* C wildtype. Presumably, this is because R25 does not
417 contain the Q154K/R mutation and instead uses another set of mutations that allows R25 to infect
418 [R8, R18, R10, R26]-heptoseless mutants.

419

420 **Discussion**

421

422 Our experiments have shown that *E. coli* C can become resistant to ΦX174 infection through
423 mutations in genes involved in the LPS biosynthesis or assembly. ΦX174 can, in turn, evolve to
424 reinfect initially resistant *E. coli* C strains by acquiring mutations in genes involved in host recognition
425 or DNA injection. Similar to ΦX174 wildtype, the evolved phages are highly host-specific and hence
426 can be used to distinguish between bacteria with different LPS structures. Such high host specificity
427 allows testing of the currently accepted LPS structure model, where LPS structures are determined by
428 the presence and absence of LPS synthesis and assembly genes. Our data on phage infectivity show

429 that LPS diversity is far greater than the current model suggests. Presumably, the modulation of LPS
430 gene activity leads to the variety of LPS phenotypes. Our findings can potentially be applied to other
431 phages that use LPS as a single or complementary receptor for host infection[56–58]. The LPS is a major
432 structural component of the outer membrane of Gram-negative bacteria[7], and its biosynthesis and
433 assembly are well known and conserved among bacterial species.
434
435 Another major finding of our study, namely that increasing phage and host diversity allows the
436 infection of hard resistant phenotypes (see **Fig. 4C**), has also been observed in a co-evolution
437 experiment between a different host-phage pair[59]. That is, phage Lambda requires at least four
438 mutations to infect the novel OmpF receptor in *E. coli* B, making it almost impossible to evolve the
439 from the wildtype phage in a single step[60]. Evolving all four mutations in one Lambda phage genome
440 first required the presence of Lambda phage evolutionary intermediates that already carried specific
441 mutations. These evolutionary intermediates arose from the infection of easy *E. coli* resistant mutants
442 (*malT* loss-of-function mutants) that could still spontaneously induce low-levels of the traditional host
443 receptor, LamB. By increasing the host diversity, the Lambda phage eventually evolved the additional
444 mutations (four in total) to overcome the hard *E. coli* mutants (*lamB* loss-of-function mutants)[59,61].
445 Similarly, we showed that the successful infection of *waaG*, *galU*, *rfaH*, and *waaP*/*pssA* resistant strains
446 became accessible by increasing host and phage diversity.
447
448 The use of bacteriophage ΦX174 could be a promising avenue for human and animal health therapies
449 (either in cocktails or in complement with antibiotics). The considerable knowledge acquired from
450 decades of research on its structure, life cycle, and evolution makes ΦX174 a good candidate for health
451 applications. Its safety has also been clinically studied and approved by the FDA[62,63]. Currently, the
452 preferred approach to phage therapy is the isolation of phages from environmental samples that can
453 infect specific bacterial pathogens[64]. However, finding new phages is often time-consuming. The
454 isolation, characterization, and adaptation of these new phages can drastically slow their suitability for
455 therapy, and their safety should also be assessed since phages are known to carry dangerous toxins[65,66].
456 The main safety advantage of ΦX174 has also been one of the greatest issues for the potential of a
457 therapeutic agent: its high host specificity[30]. Here we show that evolution experiments can easily
458 extend the host range of ΦX174 to formerly resistant strains, unlocking its potential as a powerful
459 therapeutic. Hence, due to therapeutic potential and potential for knowledge transfer, we believe that

460 established model systems such as *E. coli* C and ΦX174 should continue to be used to investigate the
461 basis for phage resistance, and mechanisms by which it can be overcome[67–69].
462

463 ## Methods

464

465 **Bacterial and phage strains.** The ancestral *Escherichia coli* strain C used in this study differs from the
466 one uploaded on the NCBI website (GenBank accession number CP020543.1) by the presence of 9
467 additional insertions and two nucleotides' replacements (c → t at the position 1,1720,214 and g → t
468 at the position 1,190,560). The sequence of CP020543.1 was manually modified using Geneious Prime
469 (version 2020.1.2). Whole-genome re-sequencing on *E. coli* C wildtype's glycerol stock confirmed the
470 modifications. All resistant bacterial strains generated in this study are derived from our ancestral
471 *Escherichia coli* strain C. All bacteriophage strains are derived from the ancestral coliphage ΦX174
472 (GenBank accession number AF176034). AF176034 sequence was downloaded from the NCBI
473 website and manually annotated using Geneious Prime (version 2020.1.2). Whole-genome re-
474 sequencing on ΦX174 wildtype's glycerol stock showed no difference. Complete genomes of *E. coli*
475 C WT and ΦX174 WT used as references have been deposited in Zenodo (doi:
476 10.5281/zenodo.6952399). Both ancestral strains were provided by H.A. Wichman (Department of
477 Biological Sciences, University of Idaho).

478

479 **Media and growth conditions.** Phage and bacteria were grown in a shaking incubator (New
480 Brunswick™ Innova® 44) at 37˚C, 250 rpm, in LB (Lysogeny Broth, Miller) medium supplemented
481 with $CaCl_2$ and $MgCl_2$ at a final concentration of 5 mM and 10 mM, respectively. Solid LB agar (1.5 %
482 agar) was used to plate both bacteria and phages. When plating phage, top agar overlay (0.5 % agar),
483 also called SSA in this study, was supplemented with $CaCl_2$ and $MgCl_2$ at a final concentration of 5
484 mM and 10 mM respectively. Overnight incubations of both plates and cultures were set up for ~16-
485 17 hours at 37˚C. PBJ solution (Phage Buffer Juice: 2.03 % Tris-HCl, 0.61 % $MgCl_2.6H_2O$) was used
486 for serial dilutions.

487

488 **Isolation and storage of *E. coli* C strains with resistance to wildtype ΦX174.** Thirty-five *E. coli*
489 C wildtype colonies were randomly chosen from an agar plate, and each used to inoculate an
490 independent overnight liquid culture. 50 µl of each stationary phase culture was mixed with 50 µl of
491 a high titer (~10^9 pfu ml^{-1}) stock of ΦX174 wildtype lysate, immediately plated on 1.5 % agar, and
492 incubated at 37˚C overnight. From each plate, half a randomly chosen colony was used to inoculate a
493 fresh overnight LB liquid culture. Once grown, a sample from each culture was mixed with glycerol
494 saline solution and cryogenically frozen at -80˚C (giving strains *E. coli* C R1-R35). To confirm the

495 acquisition of resistance to wildtype ΦX174, the remaining half of each colony was streaked onto a
496 1.5 % LB agar plate soaked with 100 μl of the high titer ΦX174 wildtype lysate, and incubated at 37˚C
497 overnight.
498
499 **Phage lysate preparation.** Ten to twelve drops of chloroform were added to growing *E. coli* C-phage
500 co-cultures, and vortexed for at least 30 seconds (to kill the bacteria). Cultures were then centrifugated
501 at 5000 rpm for 10 min at 4˚C. Supernatants (phage lysates) were transferred to sterile 5 ml Eppendorf
502 tubes and stored at 4˚C. One millilitre of each lysate was stored with glycerol saline solution and
503 cryogenically frozen at -80˚C.
504
505 **First phage evolution experiment - Standard**. The protocol from Bono *et al.*[70] was adapted to
506 evolve phages that can infect resistant *E. coli* C strains. Of R1-R35 – the 35 *E. coli* C strains resistant
507 to ΦX174 wildtype, see above – 31 were used for the first phage evolution experiment (excluding R1,
508 R3, R15, and R19; see **Results** and **Text S1**). Thirty-one ΦX174 lineages were each founded by
509 ΦX174 wildtype and serially transferred in cultures containing a mix of *E. coli* C wildtype (permissive
510 strain) and one resistant *E. coli* C strain (non-permissive strain; R2-R35). For each transfer, permissive
511 and non-permissive bacteria were grown separately until they reached log phase, then mixed in at a
512 specific ratio depending on the growth of the non-permissive strain (see **Figs. 3A & S4** and
513 **Supplementary Methods**), to a final volume of 5 ml. At each transfer, freshly prepared susceptible
514 cells were infected by ΦX174 at MOI_{input} ~ 0.1. Infected cultures were shaken at 250 rpm, 37˚C, for
515 three hours. Phage lysates were isolated as described in **Phage lysate preparation**. Phage lysates from
516 the previous day were used to inoculate the fresh bacterial mixes the next day. Transfers continued
517 until phages were found to infect their corresponding resistant *E. coli* C strain, or until 21 transfers
518 were reached. Three control lines were also run in parallel, by transferring ΦX174 at MOI_{input} ~ 0.1 in
519 a culture containing *E. coli* C wildtype only.
520
521 **Second phage evolution experiment – Increased diversity.** Four independent ΦX174 lineages
522 were founded by a phage cocktail made of (i) the wildtype ΦX174 and (ii) all isogenic ΦX174 strains
523 that successfully re-infected their corresponding resistant strains during the first phage evolution
524 experiment, at a roughly equal number of plaque forming units (PFU). Fourteen isogenic phage strains
525 were used: ΦX174 R4 T7, ΦX174 R5 T2, ΦX174 R8 T6, ΦX174 R10 T6, ΦX174 R13 T6, ΦX174
526 R18 T4, ΦX174 R19 T1, ΦX174 R20 T5, ΦX174 R21 T1, ΦX174 R24 T1, ΦX174 R26 T1, ΦX174

527 R27 T1, ΦX174 R29 T1, and ΦX174 R31 T1. Phages infecting R5 and R19 were used for the cocktail
528 but removed from the mutational analysis (see **Text S1** and **Table S4**). Each lineage was transferred
529 daily for up to four days, on non-evolving host cultures containing (i) *E. coli* C wildtype, (ii) the 14
530 host strains (see **Text S1** and **Table S4**) for which resistance had been overcome (permissive hosts),
531 and (iii) an excess of the still-resistant strain of interest (non-permissive host). For the non-permissive
532 host, we used R6 (*waaP/pssA* mutant), R22 (*galU* mutant), R25 (*rfaH* mutant), or R28 (*waaG* mutant;
533 see **Table S1**). *E. coli* C R22 and R28 were chosen as representatives of the *galU* and *waaG* mutants,
534 respectively. Each bacterial strain (permissive and non-permissive) was grown separately in LB liquid
535 culture for one hour (37˚C, 250 rpm), then pooled at roughly equal number of colony forming units
536 The resistant strain of interest was added in excess to give a final volume of 4 ml. Infected cultures
537 were initiated by adding the phage cocktail (MOI_{input} ~ 0.1), shaken at 250 rpm, 37˚C, for 5 hours (see
538 **Fig. 3B**). Phage lysates were isolated as described in **Phage lysate preparation**. Phage lysates from
539 the previous day were used to inoculate the fresh bacterial mixes the next day. This process was
540 repeated until phages were found to infect their corresponding resistant *E. coli* C strains, or until four
541 transfers had been completed. See **Supplementary Methods** for a detailed version of the protocol.
542
543 **Third evolution experiment – Increased diversity and generations.** Two independent ΦX174
544 lineages were founded by the same phage cocktail used in the second phage evolution experiment.
545 Protocol from the second evolution experiment was adjusted to reduce the amount of time necessary
546 to retrieved the desired phages. We increased the number of lineages' transfers per day from one to
547 four, for a total of four days (16 transfers). *E. coli* C R6 (*waaP/pssA* mutant) and R25 (*rfaH* mutant,
548 see **Table S1**) were used as non-permissive hosts. After reaching their exponential log phase, bacterial
549 strains (except the non-permissive hosts) were mixed depending on their growth (**Figs. 3C & S4**,
550 **Supplementary Methods**). New host cultures were kept in exponential growth phase independently
551 by transferring every hour 1:5 of the volume (1ml) in fresh LB pre-heated at 37˚C (see **Fig. 3C**).
552 Before each transfer, all host cultures were mixed together. Infected cultures were started by adding
553 the phage cocktail to the final host mix at MOI_{input} ~ 0.1, shaken at 250 rpm, 37˚C, for one hour. After
554 that, 1:15 of the volume of each infected culture was transferred in freshly mixed bacterial cultures
555 and infection continued for one hour (see **Fig. 3C**). This step was repeated for a total of four transfers.
556 The final (fourth) transfer lasted for two hours. All transfers completed on the same day involved
557 transferring both phage and bacteria; on every fourth transfer, supernatants were collected and only
558 phage transferred. Phage lysates were isolated as described in **Phage lysate preparation**. Phage lysates

559 from the previous day were used to inoculate the first fresh bacterial mixes the next day. See
560 **Supplementary Methods** for a detailed version of the protocol.
561
562 **Isolation of evolved ΦX174 strains from evolution experiments.** Top agar overlays were prepared
563 by mixing 100 μl of undiluted phage lysates with 200 μl of overnight culture of the corresponding
564 resistant *E. coli* C strain in 4 ml SSA. Plates were incubated inverted at 37°C for ~16-17 hours. An
565 isolated plaque was chosen randomly for each phage lysate to infect cultures of the corresponding
566 resistant *E. coli* C strains (in exponential growth state) incubated at 37°C, 250 rpm, for 5 hours. Phage
567 lysates were isolated as described in **Phage lysate preparation**. Phage isolates were re-isolated from
568 single plaques a second time from their glycerol stocks. See **Supplementary Methods** for a detailed
569 version of the protocol.
570
571 **Determination of the evolved phages' host range by spotting assays**
572 *Method 1*. Each top agar overlay was prepared by mixing 200 μl of an *E. coli* C strain from stationary
573 phase culture in 4 ml SSA. Then, 3 μl of each undiluted evolved phage lysate (between 10^7 and 10^9
574 pfu ml^{-1}) was dropped at the surface. *Method 2*. Each top agar overlay was prepared by mixing a volume
575 of each phage lysate in 4 ml SSA at a final concentration of ~10^7 pf ml^{-1}. Then, 3 μl of both undiluted
576 and ten-fold diluted of each *E. coli* C strain (from overnight culture) were dropped onto the surface
577 with a pipette. Plates were incubated inverted at 37°C for ~17 hours. *E. coli* C wildtype was used as a
578 positive control (permissive strain), and *E. coli* K-12 MG1655 as a negative control (non-permissive
579 strain). A bacterial host strain was classified as sensitive only when signs of lysis were detected using
580 both methods, in at least two (of three) replicates per method. A phage-bacterium combination that
581 yielded different results between the two methods was tested in standard plaque assays (see
582 **Supplementary Methods**). Finally, the host strain was classified as sensitive if plaques was observed
583 at both dilutions.
584
585 **Data visualisation.** The hierarchical agglomerative clustering analysis (Clustermap **Fig. 6**), the
586 heatmap (**Fig. S3**), and growth curves (**Fig. S4**) were generated using the default settings of the
587 Seaborn library (version 0.11.2) for Python (version 3.7.4). All schematic drawings (**Figs. 1-4, S1 and**
588 **S2**) were created with BioRender.com. The Lollipop plot (**Fig. 5A**) was generated using trackViewer
589 Vignette: lollipopPlot (Lolliplot) in R (version 1.27.11).

590

591 **Whole genome re-sequencing.**

592 *Bacteria.* Samples were prepared for whole genome re-sequencing from 1 mL of stationary-phase
593 culture. Genomic DNA was extracted using the Wizard® Genomic DNA purification Kit (Promega,
594 Germany). Extracted DNA was tested for quality, pooled, and sequenced by the Max-Planck Institute
595 for Evolutionary Biology (Plön, Germany) using an Illumina Nextera DNA Flex Library Prep Kit to
596 produce 150 bp paired-end reads[71].

597

598 *Phage.* ΦX174 samples were prepared for whole genome re-sequencing from 1 mL of phage lysate.
599 Genomic DNA was extracted using the QIAprep Spin Miniprep Kit (QIAGEN), then amplified by
600 performing 20 cycles of PCR using Q5® High-Fidelity 2X Master Mix (NEB). The primers used for
601 amplification of the ΦX174 genome are listed in **Table S6**. DNA samples were tested for quality,
602 pooled, and sequenced by the Max-Planck Institute for Evolutionary Biology (Plön, Germany).
603 Sequencing was performed using an Illumina MiSeq DNA Flex Library Prep Kit to produce 150 bp
604 paired-end reads[71].

605

606 The quality of the sequencing output from bacteria and phages was controlled using *FastQC* version
607 0.11.8. Reads were trimmed using *Trimmomatic*, assembled and analysed using the *breseq* pipeline
608 (version 0.33.2[72–74]) and Geneious Prime (version 2020.1.2).

609

610 **Sanger sequencing of ΦX174 *F* and *H* genes.** Using the ΦX174 genomic DNA extracted above
611 as templates, the *F* and *H* genes were amplified by 35 cycles of PCR using Phusion® High-Fidelity
612 PCR Master Mix with HF Buffer (ThermoFisher). Primers used for this purpose are listed in **Table**
613 **S6**. Then, Sanger sequencing was performed using sequencing primers (**Table S6**) at the Max-Planck
614 Institute for Evolutionary Biology (Plön, Germany). Sequencing results were assembled and analysed
615 with Geneious Prime (version 2020.1.2).

616

617 **Data avalaibility**

618

619 *Whole-genome and Sanger sequencing results.* Complete genomes of *E. coli* C WT and ΦX174 WT used as
620 references, and raw sequencing reads used to generated the **Tables S1-5** have been deposited in
621 Zenodo (doi: 10.5281/zenodo.6952399).

Growth curves. Raw OD measurements used to generated **Fig. S4** have been deposited in in Zenodo (doi: 10.5281/zenodo.6952399).

Hierarchical agglomerative clustering and heatmap data. Pictures and raw data used to generate **Figs. 6** and **S3** have been deposited in Zenodo (doi: 10.5281/zenodo.6952399).

627 **Supplementary Text S1**

628

629 *Bacteria and phage isolates that were excluded from downstream analyses*. We removed four bacterial strains (*E.*
630 *coli* C R1, R3, R15, and R19) and two evolved phage strains (ΦX174 R5 T2 and ΦX174 R19 T1) from
631 both mutational and phenotypical analyses. The reasons behind these exclusions are outlined below.

632

633 *Bacteria*. We found that both *E. coli* C R3 and R15 were not isogenic. While whole genome re-
634 sequencing from their respective glycerol stocks showed only a single mutation in *galE*, whole genome
635 re-sequencing performed on colony re-streaks showed that additional mutations were systematically
636 associated with the single mutation in *galE* (**Tables S4 and S5**). *E. coli* C R1 displayed an unstable
637 resistant phenotype using the spotting assay *method 1* (see section **Determination of the evolved**
638 **phages' host range by spotting assays**). We performed phenotypic assays by plating top agar
639 overlays from overnight cultures of *E. coli* C R1 without phage. All overnight cultures were started
640 with a randomly picked single colony obtained from the glycerol stock of R1. We observed that
641 colonies of R1 made different lawn types: either "smooth" (no bacterial aggregate) or "granulous"
642 (presence of numerous bacterial aggregates), which could potentially impact phage infectivity. Finally,
643 *E. coli* C R19 was only partially resistant to ΦX174 wildtype. ΦX174 wildtype was still able to infect
644 and produced a few small clear plaques on a lawn of R19. It carries a single mutation *yajC* (locus tag
645 B6N50_17610), which encodes a periplasmic protein[75] with a putative preprotein translocase subunit
646 (Pfam e-value 2.3e-26) (see **Table S4**). While no link to the LPS biosynthesis or assembly has yet been
647 defined, *yajC* could conceivably play a role in the injection of phage DNA into the bacterium's
648 cytoplasmic membrane[76,77].

649

650 In our matrices (**Figs. 6 & S3**), *E. coli* C R32 cannot be infected by any evolved phages from the first
651 evolution experiment. It is because the phage infecting R5 was the only phage that could infect R32,
652 but was removed from the subsequent analysis (see below).

653

654 *Phage*. Since we removed R19 from the final analysis, we also removed its corresponding evolved phage
655 obtained during the first evolution experiment (ΦX174 R19 T1). We also removed the phage infecting
656 R5 (ΦX174 R5 T2) because it was not isogenic (confirmed by Sanger Sequencing). Details on their
657 respective mutations (in the *H* gene) can be found in **Table S4**.

658

659 **Supplementary Figures**

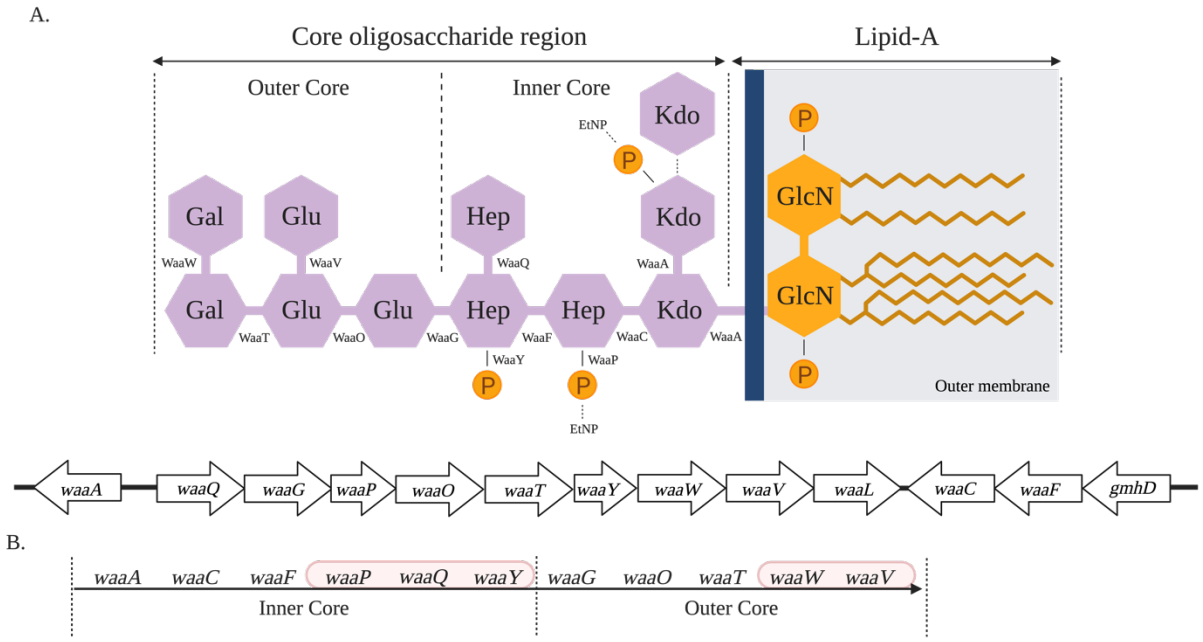

660

661 **Fig. S1. Assembly of *E. coli* rough type core LPS. A.** Organization of the chromosomal *waa* region
662 in the *E. coli C* wildtype strain. Three operons are encoded: *waaA, gmhD* and *waaQ*[18]. The *waaA* operon
663 is responsible for the incorporation of two Kdo (3-deoxy-D-*manno*-octulosonic acids) moieties to the
664 lipid A[78]. The *gmhD* operon is required for the assembly of the inner core[11] and the *waaQ* operon
665 contains all eight genes necessary to assemble the outer core[18] **B.** Inner core assembly starts first with
666 WaaA adding the two Kdo moieties to the lipid-A-IV precursor[15,11,18]. A bacterium lacking WaaA
667 activity displays sever membrane defects, resulting in the inability to form colonies[79]. Heptoses
668 residues I and II are then anchored to Kdo_2-lipid-A-IV by heptosyltransferases WaaC and WaaF,
669 respectively[11,18,80]. LPS core heptose kinases WaaP and WaaY add phosphate groups to the first and
670 second heptose residues, respectively. WaaQ adds the last heptose to the second heptose residue[11,18,80].
671 *WaaP*, *waaQ*, and *waaY* proceed in this specific order. *WaaY* cannot work without the activity of *waaQ*,
672 which cannot work without *waaP* (first red ellipse). The glucosyltransferases WaaG and WaaO start
673 the formation of the outer core by anchoring the first glucose to the second heptose residue and the
674 second glucose to the first glucose residue, respectively[81,82,18]. It has been suggested that the WaaG-
675 catalyzed reaction might be required for WaaP and WaaY substrate specificity[39]. Then, the
676 galactosyltransferases WaaT and WaaW add the first galactose to the second glucose residue and the
677 second galactose to the first galactose residue, respectively[18,83]. The completion of the outer core LPS
678 is achieved when WaaV add the third glucose to the second glucose residue. Here, *waaV* requires the

activity of *waaW* and proceed in this specific order (second red ellipse). If *waaW* is deleted, *waaV* is not functional[58,63]. Modifications of the LPS structure can lead to major phenotypic effects. In particular, the deep rough phenotype is usually associated with a strongly destabilized outer membrane, a decreased expression of some outer membrane proteins, a modification of the turgor pressure[77], and an increase of susceptibility to hydrophobic compounds such as AMPs (antimicrobial peptides), antibiotics, or bacteriocins[15,16,11,17–19]. Differences in LPS structures can also affect interactions with the host immune system[78,7] and phage resistance[9,22–24].

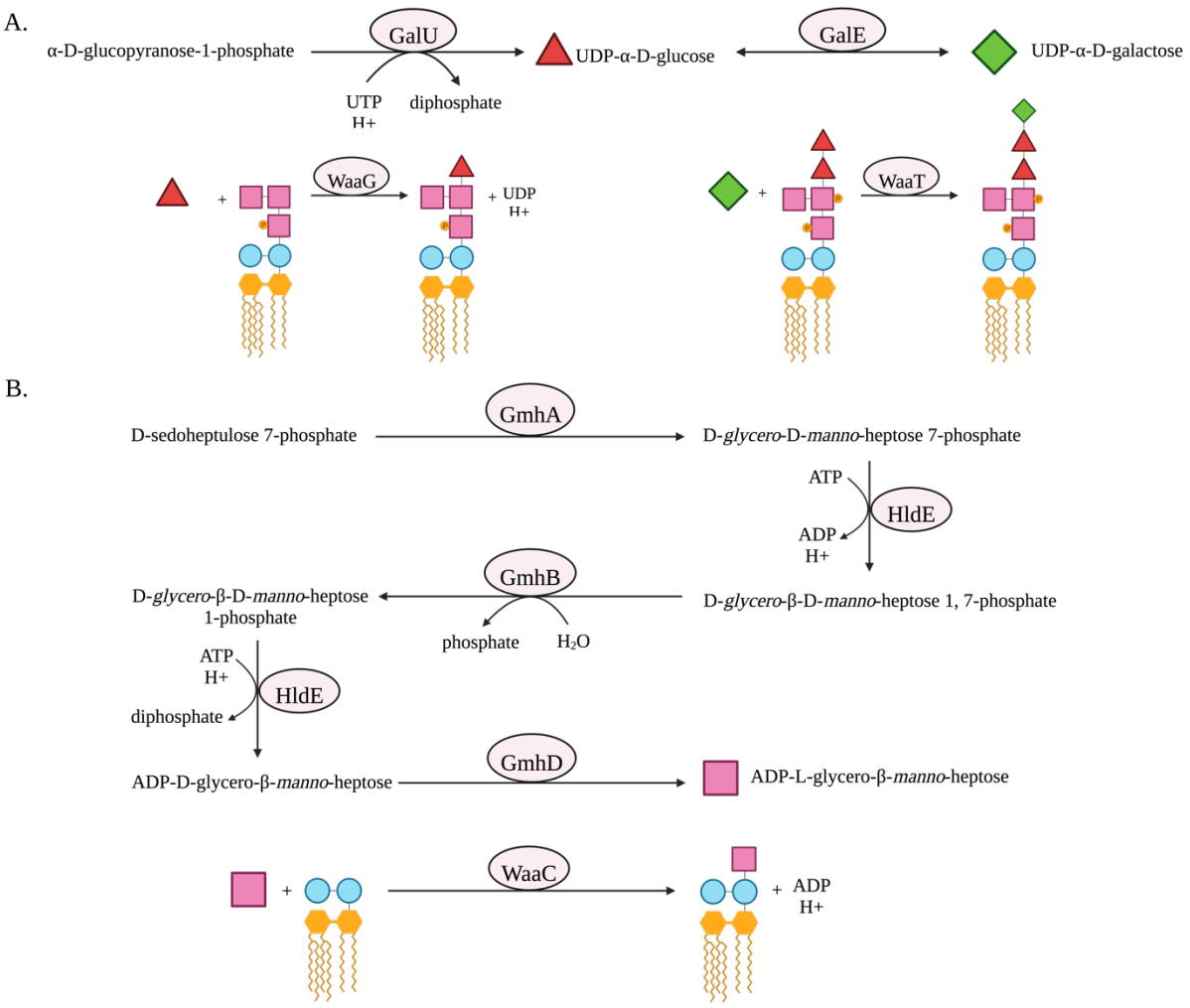

Fig S2. Biosynthesis of the core LPS glucose, galactose and heptose sugar components. A. Galactose degradation I (Leloir Pathway). GalU functions in the Leloir pathway[55,85,86]. GalU catalyses the formation of UDP-α-D-glucose from α-D-glucopyranose 1- phosphate[87]. UDP-α-D-glucose can then be incorporated into the outer core LPS by WaaG. Therefore, both Δ*galU* and Δ*waaG* mutants result in the same truncated LPS structure[88,11,87]. GalE also functions in the Leloir pathway, catalyzing the interconversion of UDP-α-D-galactose and UDP-α-D-glucose during galactose catabolism[89]. UDP-α-D-galactose is then incorporated into the outer core LPS by WaaT[83]. Therefore, both Δ*galE* and Δ*waaT* are expected to result in the same truncated LPS[90]. This figure was adapted from https://biocyc.org/ECOLI/NEW-IMAGE?type=PATHWAY&object=GALACTMETAB-PWY[91]. **B.** Then ADP-L-glycero-β-D-*manno*-heptose synthesis pathway, which involves four genes: *gmhA*, *hldE*, *gmhB* and *gmhD*. Each gene encodes a protein that catalyses the production of a heptose intermediate. The final product is ADP-L-glycero-β-D-*manno*-heptose, which is used by the

700 heptosyltransferase WaaC to build the inner core LPS[55]. Thus, deletion of one of these genes is
701 expected to result in an heptoseless, deep-rough phenotype LPS[86]. This figure is adapted from
702 https://biocyc.org/ECOLI/NEW-IMAGE?type=PATHWAY&object=PWY0-1241[91].
703

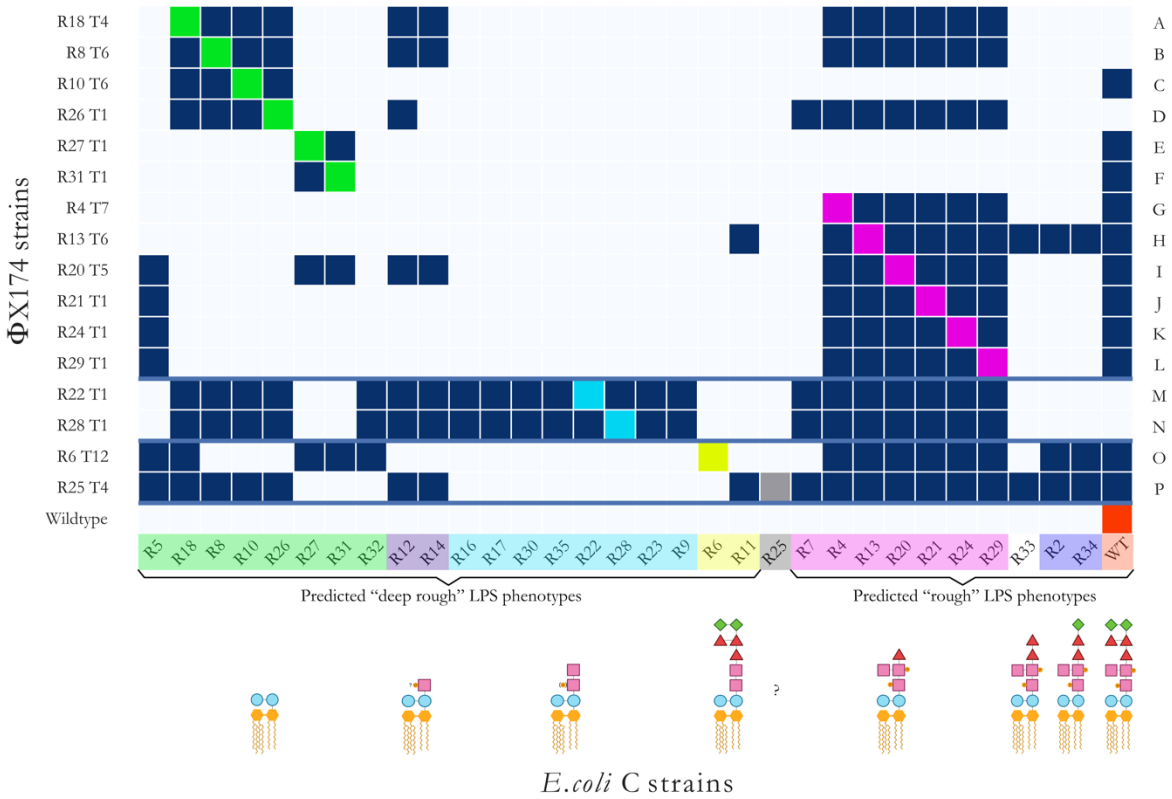

Fig. S3. Infection matrix of evolved ΦX174 phages on the 31 resistant *E. coli* C strains. The infection matrix was produced by combining the results of two spotting methods and the plaque assays (see **Methods**). *E. coli* C strains are grouped and coloured based on their predicted core LPS structures[11,12,15,18,33,34,39,55,75,80–82,84,86–88,90]. ΦX174 strains are ordered based on the predicted LPS structures they infected during the evolution experiments (A-F: overcame heptoseless *waaC* and *hldE* mutants; G-L: overcame *waaO* mutants; M-N: overcame *galU* and *waaG* mutants; O: overcame *waaP*/*pssA* mutant; P: overcame *rfaH* mutant). The solid blue lines separate the evolved phages according to the evolution experiment in which they were isolated (A-L: first; M-N: second; O-P: third). Dark blue squares=infection, light blue square=no infection, coloured square=control infection by a phage evolved on that host. R# indicates the number of the resistant strain the phage evolved on, and T# is the transfer number where plaques were first observed. "?": core LPS structure of *E. coli* C R25 (*rfaH* mutant) could not be predicted.

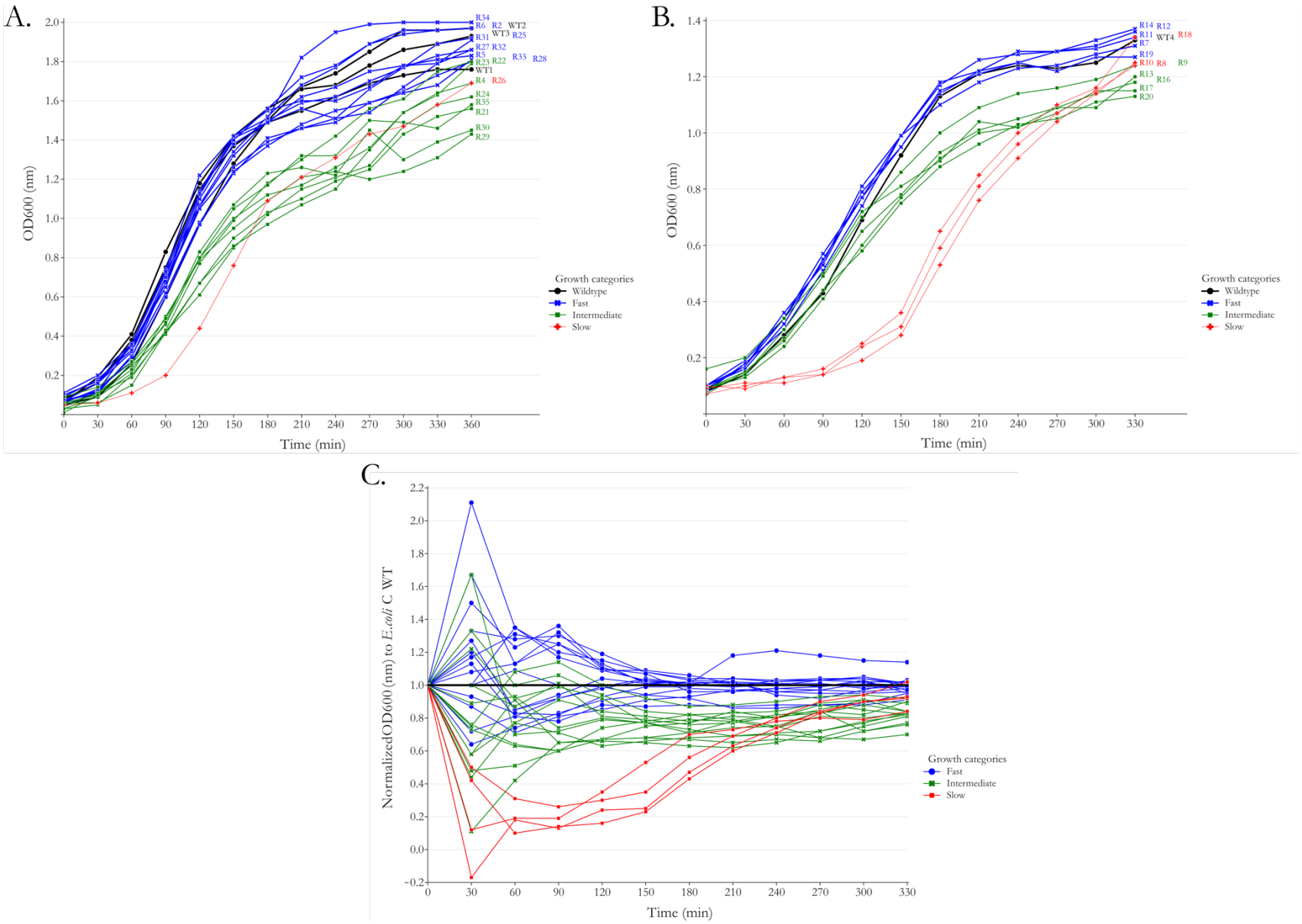
A.
OD600 (nm)
Time (min)
R34
R6
R2
WT2
WT3
R31
R25
R27
R32
R5
R33
R28
R23
R22
WT1
R4
R26
R24
R35
R21
R30
R29
Growth categories
Wildtype
Fast
Intermediate
Slow
B.
OD600 (nm)
Time (min)
R14
R12
R11
WT4
R18
R7
R19
R10
R8
R9
R13
R16
R17
R20
Growth categories
Wildtype
Fast
Intermediate
Slow
C.
NormalizedOD600 (nm) to E.coli C WT
Time (min)
Growth categories
Fast
Intermediate
Slow

717

718 **Fig. S4. *E. coli* C resistant strains can be categorized as fast, intermediate, or slow growers.** Two independent cultures of each resistant
719 strain were grown at 37°C, 250 rpm for 17 hours. 180 μl of each overnight culture was inoculated into a 1 4ml sterile tube (FALCON)
720 containing 5 ml of LB (supplemented with $CaCl_2$ and $MgCl_2$ at final concentrations of 5 mM and 10 mM, respectively). Incubation time was
721 set for 6 hours at 37°C, 250 rpm. Optical density (OD) was measured at 600nm every 30 minutes with an Ultrospec 10 (Biochrom). *E. coli* C
722 wildtype was used as a reference. The mean OD600 values at each time point for each bacterial mutant were calculated and plotted. Resistant
723 strains are categorized with respect to their growth compared to *E. coli* C wildtype. Black lines: *E. coli* C wildtype. Blue lines: resistant bacteria
724 that grew similarly to *E. coli* C wildtype ("fast growers"). Green lines: resistant strains grew somewhat more slowly than *E. coli* C wildtype and
725 fast growers ("intermediate growers"). Red lines: resistant strains that grew more slowly than *E. coli* C wildtype and intermediate growers
726 ("slow growers"). **A.** Growth curves of resistant strains R2-R6 and R21-R35. **B.** Growth curves of resistant strains R7-R20. These data
727 (mutants and controls) were collected in a separate block to those in panel A. **C.** Mean OD600 values of all resistant strains in panels A and
728 B, each normalized with respect to their corresponding *E. coli* C wildtype control.
729

730 **Supplementary Tables**

E. coli C resistant strains	Genes	Locus tags	Synonyms	Descriptions	Positions	Nucleotide changes	Amino Acid changes	Predicted LPS structure phenotypes	"Easy" or "Hard" LPS structure phenotypes?	# Experiment during which resistance was overcome or cross-infected
R2	*waaW*	*B6N50_00430* →	-	UDP-galactose--(galactosyl) LPS alpha1,2-galactosyltransferase	79,779	g→a	G267D	Rough	Easy	1
R4	*waaO*	*B6N50_00415* →	*rfaI*	UDP-D-glucose:(glucosyl)LPS α-1,3-glucosyltransferase	76,970	$(a)_{7\rightarrow6}$	L249fsTer#263[a]	Rough	Easy	1
R5	*gmhB*	*B6N50_18960* ←	-	D-glycero-beta-D-manno-heptose 1,7-bisphosphate 7-phosphatase	3,693,747	$(t)_{8\rightarrow7}$	M45fsTer#51	Deep rough	Easy	1
R6	*waaP*	*B6N50_00410* →	*rfaP*	Lipopolysaccharide core heptose(I) kinase	76,163 - 76,168	Δ6 bp	Δ(A251-A253)	Deep rough	Hard	3
	pssA	*B6N50_06070* ←	-	Phosphatidylserine synthase	1,190,560	t→g	V54V			
R7	*waaO*	*B6N50_00415* →	*rfaI*	UDP-D-glucose:(glucosyl)LPS α-1,3-glucosyltransferase	77,219 - 77,224	$(ttattt)_{2\rightarrow1}$	Δ(F332-L334)	Rough	Easy	1
R8	*hldE*	*B6N50_03700* →	*rfaE/waaE*	Bifunctional heptose 7-phosphate kinase/heptose 1-phosphate adenyltransferase	721,891 - 721,892	$(gc)_{5\rightarrow4}$	A79fs_Ter#83	Deep rough	Easy	1
R9	*waaG*	*B6N50_00405* →	*rfaG*	UDP-glucose:(heptosyl) LPS α1,3-glucosyltransferase (glucosyltransferase I)	75,073 - 75,076	Δ4 bp	G260fs_Ter#266	Deep rough	Hard	2
R10	*hldE*	*B6N50_03700* →	*rfaE/waaE*	Bifunctional heptose 7-phosphate kinase/heptose 1-phosphate adenyltransferase	721,891 - 721,892	$(gc)_{5\rightarrow4}$	A79fs_Ter#83	Deep rough	Easy	1
	CRISPR	B6N50_05180 → / ← B6N50_05185	-	Repeat region	1,023,697 - 1,023,940	Δ244 bp	Non-coding region			
R11	*waaP*	*B6N50_00410* →	*rfaP*	Lipopolysaccharide core heptose(I) kinase	75,562	g→a	W51stop	Deep rough	Easy	1
R12	*waaF*	*B6N50_00450* ←	*rfaF*	ADP-heptose--LPS heptosyltransferase II	84,376	g→a	Q30stop	Deep rough	Easy	1
R13	*waaO*	*B6N50_00415* →	*rfaI*	UDP-D-glucose:(glucosyl)LPS α-1,3-glucosyltransferase	76,255	Δ1 bp	M11fsTer#58	Rough	Easy	1
R14	*waaF*	*B6N50_00450* ←	*rfaF*	ADP-heptose--LPS heptosyltransferase II	84,081	c→t	W128stop	Deep rough	Easy	1
R16	*galU*	*B6N50_13325* ←	-	UTP--glucose-1-phosphate uridylyltransferase	2,611,994	Δ1 bp	V37fsTer#41	Deep rough	Hard	2
R17	*galU*	*B6N50_13325* ←	-	UTP--glucose-1-phosphate uridylyltransferase	2,611,409	$(g)_{4\rightarrow3}$	P232fsTer#248	Deep rough	Hard	2
R18	*waaC*	*B6N50_00445* ←	*rfaC*	ADP-heptose--LPS heptosyltransferase I	83,271	Δ1 bp	H48fsTer#71	Deep rough	Easy	1
R20	*waaO*	*B6N50_00415* →	*rfaI*	UDP-D-glucose:(glucosyl)LPS α-1,3-glucosyltransferase	77,104	g→a	W294stop	Rough	Easy	1

731

R21	*waaO*	*B6N50_00415* →	*rfaI*	UDP-D-glucose:(glucosyl)LPS α-1,3-glucosyltransferase	76,978	c→a	S252stop	Rough	Easy	1
	potH	*B6N50_15295* ←	-	Spermidine/putrescine ABC transporter permease	2,990,409	g→t	Q310K			
R22	*galU*	*B6N50_13325* ←	-	UTP--glucose-1-phosphate uridylyltransferase	2,611,590 - 2,611,600	INS 2,783,815 - 2,784,943	M168_V172ins(376)[b]	Deep rough	Hard	2
R23	*waaG*	*B6N50_00405* →	*rfaG*	UDP-glucose:(heptosyl) LPS α1,3-glucosyltransferase (glucosyltransferase I)	74,589 - 74,606	Δ18 bp	Δ(A99-E105)	Deep rough	Hard	2
R24	*waaO*	*B6N50_00415* →	*rfaI*	UDP-D-glucose:(glucosyl)LPS α-1,3-glucosyltransferase	76,970	$(a)_{7\rightarrow 6}$	L249fsTer#263	Rough	Easy	1
R25	*rfaH*	*B6N50_22865* →	-	Transcription/translation regulatory transformer protein	4,485,876	g→a	W4stop	Unknown	Hard	3
R26	*hldE*	*B6N50_03700* →	*rfaE/waaE*	Bifunctional heptose 7-phosphate kinase/heptose 1-phosphate adenyltransferase	722,353	t→c	S233P	Deep rough	Easy	1
R27	*hldE*	*B6N50_03700* →	*rfaE/waaE*	Bifunctional heptose 7-phosphate kinase/heptose 1-phosphate adenyltransferase	721,736	g→c	G27A	Deep rough	Easy	1
R28	*waaG*	*B6N50_00405* →	*rfaG*	UDP-glucose:(heptosyl) LPS α1,3-glucosyltransferase (glucosyltransferase I)	74,864	g→t	G191stop	Deep rough	Hard	2
R29	*waaO*	*B6N50_00415* →	*rfaI*	UDP-D-glucose:(glucosyl)LPS α-1,3-glucosyltransferase	76,970	$(a)_{7\rightarrow 6}$	L249fsTer#263	Rough	Easy	1
	pcoA	*B6N50_01165* ←	-	Multicopper oxidase	237,963 - 237,973	INS 1,040,936 - 1,042,273	G152_G155ins(446)			
	eutM - eutN - eutE	*[B6N50_06785] - [B6N50_06790] - [B6N50_06795]* →	-	Ethanolamine utilization protein EutM - Ethanolamine utilization protein EutN - Aldehyde dehydrogenase EutE	1,342,381 - 1,343,448	Δ1,068 bp	Δ[EutM_A58-EutE_A181][c]			
R30	*galU*	*B6N50_13325* ←	-	UTP--glucose-1-phosphate uridylyltransferase	2,611,680	c→a	E142stop	Deep rough	Hard	2
R31	*hldE*	*B6N50_03700* →	*rfaE/waaE*	Bifunctional heptose 7-phosphate kinase/heptose 1-phosphate adenyltransferase	721,736	g→c	G27A	Deep rough	Easy	1
R32	*hldE*	*B6N50_03700* →	*rfaE/waaE*	Bifunctional heptose 7-phosphate kinase/heptose 1-phosphate adenyltransferase	722,381 - 722,482	DUP 722,381-722,482 (102) bp	P242_A276dup(34)[d]	Deep rough	Easy	1
R33	*waaT*	*B6N50_00420* →	-	UDP-galactose:(glucosyl) LPS α-1,2-galactosyltransferase	78,125	g→a	W290stop	Rough	Easy	1
R34	*waaW*	*B6N50_00430* →	-	UDP-galactose--(galactosyl) LPS alpha1,2-galactosyltransferase	79,820	c→t	Q281stop	Rough	Easy	1
R35	*galU*	*B6N50_13325* ←	-	UTP--glucose-1-phosphate uridylyltransferase	2,611,872 - 2,611,880	INS 2,783,815 - 2,784,945	S75_L78ins(377)	Deep rough	Hard	2

Table S1: List of mutations found in *E. coli* C strains that are resistant to wildtype ΦX174. *E. coli* C resistant strains: R# is the strain number. Genes: name of the gene(s) in which mutations have been identified (as compared with wildtype *E. coli* C, GenBank accession CP020543.1). Locus tags: identifier of each listed gene. Synonyms: alternative gene names. Descriptions: protein product encoded by each listed gene. Positions: genomic coordinates of mutation. Nucleotide changes: observed nucleotide change. Amino acid changes: resulting change in amino acid sequence. Predicted LPS structure phenotypes: based on predicted LPS structure (see **Fig. 2**). "Easy" or "Hard" LPS structure phenotypes?: easy LPS phenotypes were overcome or could be cross-infected after the first phage evolution experiment, while hard LPS phenotypes required the second or third phage evolution experiment to be infected. "→": indicates 5'→3' direction. "INS": insertion. "DUP": duplication. "stop": stop codon. "[a]": L249fsTer#263 indicates a frameshift (fs) leading to a premature codon stop (Ter); the position of the premature stop codon is in parentheses. "[b]": M168_V172ins(376) indicates an insertion; the two flanking amino acids are separated by a "_" and followed by the number of inserted amino acids in parentheses. "[c]": Δ[EutM_A58-EutE_A181] indicated a long deletion starting from EutM to EutE. P242_A276dup(34) indicates a duplication; the two flanking amino acids are separated by a "_" and followed by the number of duplicated amino acids in parentheses.

ΦX174 strains	Evolution experiment #	Gene mutated in the corresponding *E. coli* C resistant strains	Mutants sensitive to the evolved ΦX174 strain infection	Gene mutated in ΦX174 strains	Descriptions	Positions	Nucleotide changes	Amino acid changes	Mutations present in a control lineage?
R21 T1	1	*waaO*	R5, R4, R13, R20, R21, R24, R29, WT	*F*	Capsid protein	1,347	a→g	D116G	No
				H	Minor spike protein	3,132	g→a	A68T	No
R24 T1	1	*waaO*	R5, R4, R13, R20, R21, R24, R29, WT	*F*	Capsid protein	1,346	g→a	D116S	No
				F	Capsid protein	1,347	a→g	D116S	No
R26 T1	1	*hldE*	R18, R8, R10, R26, R12, R7, R4, R13, R20, R21, R24, R29	*F*	Capsid protein	1,460	c→a	Q154K	No
				H	Minor spike protein	3,132	g→a	A68T	No
R27 T1	1	*hldE*	R27, R31, WT	*H*	Minor spike protein	3,202	g→t	G91V	No
R29 T1	1	*waaO*	R5, R4, R13, R20, R21, R24, R29, WT	*F*	Capsid protein	1,346	g→a	D116S	No
				F	Capsid protein	1,347	a→g	D116S	No
R31 T1	1	*hldE*	R27, R31, WT	*H*	Minor spike protein	3,202	g→t	G91V	No
R18 T4	1	*waaC*	R18, R8, R10, R26, R12, R14, R4, R13, R20, R21, R24, R29	*F*	Capsid protein	1,307	t→c	Y103H	No
				F	Capsid protein	1,461	a→g	Q154R	No
				H	Minor spike protein	3,132	g→a	A68T	No
R20 T5	1	*waaO*	R5, R27, R31, R12, R14, R4, R13, R20, R21, R24, R29, WT	*F*	Capsid protein	1,354	t→a	N118K	No
				H	Minor spike protein	3,132	g→a	A68T	No
R8 T6	1	*hldE*	R18, R8, R10, R26, R12, R14, R4, R13, R20, R21, R24, R29	*F*	Capsid protein	1,307	t→c	Y103H	No
				F	Capsid protein	1,461	a→g	Q154R	No
				F	Capsid protein	3,132	g→a	A68T	No
R10 T6	1	*hldE*	R18, R8, R10, R26, WT	*F*	Capsid protein	1,317	a→g	H106R	No
				F	Capsid protein	1,460	c→a	Q154K	No
R13 T6	1	*waaO*	R11, R4, R13, R20, R21, R24, R29, R33, R2,	*F*	Capsid protein	2,015	g→c	D339H	No
R4 T7	1	*waaO*	R4, R13, R20, R21, R24, R29, WT	*F*	Capsid protein	1,301	a→g	T101A	Yes (in C1 T21)
				F	Capsid protein	1,347	a→g	D116G	No
				F	Capsid protein	2,085	c→t	A362V	No
R22 T1	2	*galU*	R18, R8, R10, R26, R32, R12, R14, R16, R17, R30, R35, R22, R28, R23, R9, R7, R4, R13, R20, R21, R24, R29	*F*	Capsid protein	1,307	t→c	Y103H	No
				F	Capsid protein	1,317	a→g	H106R	No
				F	Capsid protein	1,461	a→g	Q154R	No
				H	Minor spike protein	3,132	g→a	A68T	No
R28 T1	2	*waaG*	R18, R8, R10, R26, R32, R12, R14, R16, R17, R30, R35, R22, R28, R23, R9, R7, R4, R13, R20, R21, R24, R29	*F*	Capsid protein	1,307	t→c	Y103H	No
				F	Capsid protein	1,317	a→g	H106R	No
				F	Capsid protein	1,461	a→g	Q154R	No
				H	Minor spike protein	3,132	g→a	A68T	No
R25 T4	3	*rfaH*	R5, R18, R8, R10, R26, R12, R14, R25, R11, R7, R4, R13, R20, R21, R24, R29, R33, R2, R34, WT	*F*	Capsid protein	1,301	a→g	T101A	Yes (in C1 T21)
				F	Capsid protein	1,304	g→c	G102R	No
				F	Capsid protein	1,347	a→g	D116G	No
				H	Minor spike protein	3,132	g→a	A68T	No
R6 T12	3	*waaP*	R5, R18, R27, R31, R32, R6, R4, R13, R20, R21, R24, R29, R2, R34, WT	*F*	Capsid protein	1,727	c→t	L243F	No
				F	Capsid protein	2,015	g→c	D339H	No
				H	Minor spike protein	3,132	g→a	A68T	No
				H	Minor spike protein	3,154	c→t	A75V	No

748 **Table S2: List of mutations identified in ΦX174 evolved isolates.** ΦX174 strains: R# is the corresponding resistant strain number and
749 T# is the transfer number where plaques were observed for the first time on the given resistant strain. Evolution experiment #: experiment
750 number from which the evolved phages were isolated. Mutants sensitive to the evolved ΦX174 strains infection: list of all resistant strains
751 that a specific phage strain can infect (See **Figs. 6 and S4**). Descriptions: names of proteins encoded by the listed genes. Positions: genomic
752 coordinates of mutation (according to GenBank accession number AF176034.1). Nucleotide changes: observed nucleotide change. Amino
753 acid changes: resulting change in amino acid sequence. "→": indicates 5'→3' direction. Mutations present in a control lineage?: indicates
754 mutations that were observed in at least one control lineage (see **Methods**).
755

ΦX174 populations	Gene mutated in the corresponding *E. coli* C resistant strains	Gene mutated in ΦX174 strains	Descriptions	Positions	Nucleotide changes	Amino acid changes	Frequencies (%)	Mutations present in a control lineage?
C1 T21	None (WT)	*F*	Capsid protein	1,301	a→g	T101A	69,8	-
		F	Capsid protein	1,965	g→a	G322D	70,9	-
C2 T21	None (WT)	*F*	Capsid protein	1,968	a→g	N323S	17,8	-
		F	Capsid protein	2,277	c→t	T426I	56,7	-
C3 T21	None (WT)	*F*	Capsid protein	2,277	c→t	T426I	5,7	-
		F	Capsid protein	2,280	c→t	S247L	80,7	-
R2 T21	*waaW*	*F*	Capsid protein	1,965	g→a	G322D	19,0	Yes (in C1 T21)
		F	Capsid protein	2,276	a→g	T426A	30,4	No
		F	Capsid protein	2,279	t→c	S427P	10,9	No
		F	Capsid protein	2,280	c→t	S247L	30,9	Yes (in C3 T21)
R5 T21	*gmhB*	NA	NA	NA	NA	NA	NA	NA
R7 T21	*waaO*	*F*	Capsid protein	2,279	t→c	S427P	5,4	
		F	Capsid protein	2,280	c→t	S247L	93,2	Yes (in C3 T21)
R9 T21	*waaG*	*F*	Capsid protein	2,280	c→t	S247L	100	Yes (in C3 T21)
R11 T21	*waaP*	NA	NA	NA	NA	NA	NA	NA
R12 T21	*waaF*	*F*	Capsid protein	2,280	c→t	S247L	100	Yes (in C3 T21)
R14 T21	*waaF*	*F*	Capsid protein	2,280	c→t	S247L	93,5	Yes (in C3 T21)
R16 T21	*galU*	*F*	Capsid protein	2,280	c→t	S247L	100	Yes (in C3 T21)
R17 T21	*galU*	*F*	Capsid protein	2,279	t→c	S427P	6,7	No
		F	Capsid protein	2,280	c→t	S247L	93,1	Yes (in C3 T21)
R23 T21	*waaG*	*F*	Capsid protein	1,301	a→g	T101A	5,6	Yes (in C1 T21)
		F	Capsid protein	2,280	c→t	S247L	91,6	Yes (in C3 T21)
R30 T21	*galU*	*F*	Capsid protein	2,279	t→c	S427P	7,9	No
		F	Capsid protein	2,280	c→t	S247L	90,0	Yes (in C3 T21)
R32 T21	*hldE*	*F*	Capsid protein	2,276	a→g	T426A	29,6	No
		F	Capsid protein	2,277	c→t	T426I	6,8	Yes (in C2 T21 and C3
		F	Capsid protein	2,280	c→t	S247L	61,9	Yes (in C3 T21)
R33 T21	*waaT*	*F*	Capsid protein	2,276	a→g	T426A	42,9	No
		F	Capsid protein	2,277	c→t	T426I	14,8	Yes (in C2 T21 and C3
		F	Capsid protein	2,280	c→t	S247L	41,7	Yes (in C3 T21)
		*A/A**	Replication-associated protein/protein A*	4,817	c→t	D279D/D107D	12,8	No
R34 T21	*waaW*	NA	NA	NA	NA	NA	NA	NA
R35 T21	*galU*	*F*	Capsid protein	1,301	a→g	T101A	19,1	Yes (in C1 T21)
			Capsid protein	1,649	c→t	R217C	8,0	No
			Capsid protein	2,179	g→t	Q393H	6,8	No
			Capsid protein	2,280	c→t	S247L	82,9	Yes (in C3 T21)

756

757 **Table S3: List of mutations found in the evolved ΦX174 populations that did not infect their corresponding *E. coli* C resistant**
758 **strains.** ΦX174 populations: R# is the corresponding resistant strain number and T# is the transfer number where plaques were observed
759 for the first time on the given resistant strain. Descriptions: names of proteins encoded by the listed genes. Positions: genomic coordinates
760 of mutation (according to GenBank accession number AF176034.1). Nucleotide changes: observed nucleotide change. Amino acid changes:
761 resulting change in amino acid sequence. "→": indicates 5'→3' direction. Frequencies (%): frequency of a given mutation in the phage
762 population. Mutations present in a control lineage?: indicates mutations that were observed in at least one control lineage (see **Methods**).
763 NA: no data available.
764

Excluded *E. coli* C resistant strains	Genes	Locus tags	Synonyms	Descritptions	Positions	Nucleotide changes	Amino Acid changes	Predicted LPS structure phenotypes
R1	*waaV*	*B6N50_00435* →	-	UDP-glucose:(Glucosyl) LPS β1,3-	80,534	$(t)_{7\rightarrow 6}$	F149fsTer#158[a]	Rough
	galE	*B6N50_15815* →	-	UDP-glucose 4-epimerase	3,096,098 - 3,096,107	Δ10 bp	T228fsTer#233	
R3	*galE*	*B6N50_15815* →	-	UDP-glucose 4-epimerase	3,095,443	g→a	G10D	Rough
R15	*galE*	*B6N50_15815* →	-	UDP-glucose 4-epimerase	3,096,191	c→a	Y259stop	Rough
R19	*yajC*	*B6N50_17610* ←	-	Preprotein translocase subunit	3,447,574	Δ1 bp	G18fsTer#23	Wildtype

ΦX174 strains	Evolution experiment #	Gene mutated in the corresponding *E. coli*	Gene mutated in ΦX174 strains	Descriptions	Positions	Nucleotide changes	Amino acid changes	Mutations present in a control lineage ?
R19 T1	1	*yajC*	*H*	Minor spike protein	3,781	c→a	S284Y	No
R5 T2	1	*gmhB*	*H*	Minor spike protein	3,169	c→t	G80V	No

765

766 **Table S4: List of all *E. coli* C and evolved ΦX174 isolates excluded from the analysis.** *E. coli* C resistant strains: R# is the bacterial
767 resistant strain number. Genes: name of gene mutated. Locus tags: identifier of each listed gene. Synonyms: alternative gene names.
768 Descriptions: protein product encoded by each listed gene. Positions: genomic coordinates of mutation. Nucleotide changes: observed
769 nucleotide change. Amino acid changes: resulting change in amino acid sequence. Predicted LPS structure phenotypes: based on predicted
770 LPS structure (see **Fig. 2**). "→": indicates 5'→3' direction. "stop": stop codon. "[a]": F149fsTer#158 indicates a frameshift (fs) leading to a
771 premature codon stop (Ter); the position of the premature stop codon is in parentheses. ΦX174 strains: R# is the corresponding resistant
772 strain number and T# is the transfer number where plaques were observed for the first time on the given resistant strain. Evolution
773 experiment #: experiment number where the evolved phages were obtained. Descriptions: names of proteins encoded by the listed genes.
774 Positions: genomic coordinates of mutation (according to GenBank accession number AF176034.1). Nucleotide changes: observed
775 nucleotide change. Amino acid changes: resulting change in amino acid sequence. Mutations present in a control lineage?: indicates mutations
776 that were observed in at least one control lineage (see **Methods**).

777

E. coli C resistant strains	Replicate #	Genes	Locus tags	Descritptions	Positions	Nucleotide changes	Amino Acid changes	Predicted LPS structure phenotypes
R3	1	*gltD*	*B6N50_02830* ←	Glutamate synthase subunit gltD	555,954	t→c	Y318C	Rough
		galE	*B6N50_15815* →	UDP-glucose 4-epimerase	3,095,443	g→a	G10D	
R3	2, 3, 5, 9, 10	*WaaT*	*B6N50_00420* →	UDP-galactose:(glucosyl) LPS α-1,2-galactosyltransferase	77,302	$(a)_{6\rightarrow5}$	K16fsTer#23[a]	Rough
		gltD	*B6N50_02830* ←	Glutamate synthase subunit gltD	555,954	t→c	Y318C	
		-	-	Hypothetical protein	2,147,627	c→t	Q793stop	
		galE	*B6N50_15815* →	UDP-glucose 4-epimerase	3,095,443	g→a	G10D	
R3	4	*oppB*	*B6N50_13280* ←	Murein tripeptide ABC transporter/inner membrane subunit	2,600,004	g→a	A211V	Deep rough
		galU	*B6N50_13325* ←	UTP--glucose-1-phosphate uridylyltransferase	2,611,933	Δ1 bp	I57fsTer#86	
		galE	*B6N50_15815* →	UDP-glucose 4-epimerase	3,095,443	g→a	G10D	
R3	6	*hldD*	*B6N50_00455* ←	ADP-L-glycero-D-mannoheptose-6-epimerase	84,986	g→t	Y140stop	Rough
		galE	*B6N50_15815* →	UDP-glucose 4-epimerase	3,095,443	g→a	G10D	
R3	7	*galE*	*B6N50_15815* →	UDP-glucose 4-epimerase	3,095,443	g→a	G10D	Rough
		galT	*B6N50_15820* →	Galactose-1-phosphate uridylyltransferase	3,097,396	t→c	L319P	
R3	8	*gltD*	*B6N50_02830* ←	Glutamate synthase subunit gltD	555,954	t→c	Y318C	Rough
		-	-	Hypothetical protein	2,147,627	c→t	Q793stop	
		galE	*B6N50_15815* →	UDP-glucose 4-epimerase	3,095,443	g→a	G10D	

778

R15	1	*galP*	*B6N50_04295* ←	Galactose-proton symporter	835,258	a→g	F405L	Rough
		galE	*B6N50_15815* →	UDP-glucose 4-epimerase	3,096,191	c→a	Y259stop	
R15	2	*WaaT*	*B6N50_00420* →	UDP-galactose:(glucosyl) LPS α-1,2-galactosyltransferase	77,590	g→t	E112stop	Rough
		galE	*B6N50_15815* →	UDP-glucose 4-epimerase	3,096,191	c→a	Y259stop	
R15	3 - 6	*waaW*	*B6N50_00430* →	UDP-galactose--(galactosyl) LPS alpha1,2-galactosyltransferase	79,764	t→g	L262R	Rough
		galE	*B6N50_15815* →	UDP-glucose 4-epimerase	3,096,191	c→a	Y259stop	
R15	7	*galP*	*B6N50_04295* ←	Galactose-proton symporter	836,442	g→t	S10stop	Rough
		galE	*B6N50_15815* →	UDP-glucose 4-epimerase	3,096,191	c→a	Y259stop	
R15	8	*galP*	*B6N50_04295* ←	Galactose-proton symporter	835,353	a→g	L373P	Rough
		galE	*B6N50_15815* →	UDP-glucose 4-epimerase	3,096,191	c→a	Y259stop	
R15	9	*galE*	*B6N50_15815* →	UDP-glucose 4-epimerase	3,096,191	c→a	Y259stop	Rough
R15	10	*galP*	*B6N50_04295* ←	Galactose-proton symporter	835,170	c→t	W434stop	Rough
		galE	*B6N50_15815* →	UDP-glucose 4-epimerase	3,096,191	c→a	Y259stop	

Table S5: List of the additional mutations associated with *galE* mutations. *E. coli* C resistant strains: R# is the bacterial resistant strain number. Descriptions: protein product encoded by each listed gene. Positions: genomic coordinates of mutation. Nucleotide changes: observed nucleotide change. Amino acid changes: resulting change in amino acid sequence. Predicted LPS structure phenotypes: based on predicted LPS structure (see **Fig. 2**). "→": indicates 5'→3' direction. "stop": stop codon. "[a]": K16sTer#23 indicates a frameshift (fs) leading to a premature codon stop (Ter); the position of the premature stop codon is in parentheses.

Name	Sequence (5'→3')	Binding Region	Tm 2Q5	Ta 2Q5	Purpose
ΦX174_2361_r	TCGCTTGGTCAACCCCTCAG	2342-2361	70˚C	71˚C	ΦX174 Whole genome amplification
ΦX174_2362_f	AGCGCGGTAGGTTTTCTGCT	2362-2382	70˚C		
ΦX174_399_r	CTTGACTCATGATTTCTTACC	379-399	58˚C	59˚C	ΦX174 Whole genome amplification
ΦX174_400_f	TTACTGAACAATCCGTACGTTTC	400-422	62˚C		

Name	Sequence (5'→3')	Binding Region	Tm Phusion (buffer HF)	Ta Phusion (buffer HF)	Purpose
ΦX174_F_fw	CGCTCGTCTTTGGTATGTAGGTGG	928-951	65˚C	68˚C	Amplification of ΦX174's *F* gene
ΦX174_F_rv	AGCGGCGTTGACAGATGTATCC	2580-2601	65˚C		Amplification of ΦX174's *F* gene
ΦX174_F_fw2	GTTGCGAGGTACTAAAGGCAAGCG	898-921	66˚C	68˚C	Amplification of ΦX174's *F* gene
ΦX174_F_rv2	CTGGAGTAACAGAAGTGAGAACCAGC	2245-2470	65˚C		Amplification of ΦX174's *F* gene
ΦX174_F_fw_short	CGTCTTTGGTATGTAGGTGG	932-951	57˚C	61˚C	Amplification of ΦX174's *F* gene
ΦX174_F_rv_short	CGGCGTTGACAGATGTATC	2581-2599	58˚C		Amplification of ΦX174's *F* gene
ΦX174_H_fw	CAAGGACTGTGTGACTATTGACGTCC	2763-2788	65˚C	68˚C	Amplification of ΦX174's *H* gene
ΦX174_H_rv	GCCTCTACGCGATTTCATAGTGGAG	4490-4514	65˚C		Amplification of ΦX174's *H* gene
ΦX174_H_fw2	CGCTACTAAATGCCGCGGATTGG	2847-2869	66˚C	67˚C	Amplification of ΦX174's *H* gene
ΦX174_H_rv2	GCCTCCAGCAATCTTGAACACTC	4467-4489	64˚C		Amplification of ΦX174's *H* gene
ΦX174_H_fw_short	GACTGTGTGACTATTGACGTCC	2767-2788	60˚C	61˚C	Amplification of ΦX174's *H* gene
ΦX174_H_rv_short	GCCTCTACGCGATTTCATAG	4495-4514	58˚C		Amplification of ΦX174's *H* gene

Name	Sequence (5'→3')	Binding Region	Tm	Ta	Purpose
ΦX174_F_Sanger_fw	CCTCATCGTCACGTTTATGG	1217-1236	58˚C	56˚C	Sanger sequencing of ΦX174's *F* gene
ΦX174_F_Sanger_fw2	ACCGATATTGCTGGCGAC	1934-1951	59˚C	56˚C	Sanger sequencing of ΦX174's *F* gene
ΦX174_F_Sanger_rv	GGCGTTATAACCTCACACTC	2294-2313	58˚C	56˚C	Sanger sequencing of ΦX174's *F* gene
ΦX174_F_Sanger_rv2	GGCGAGAAAGCTCAGTCTC	1529-1547	60˚C	56˚C	Sanger sequencing of ΦX174's *F* gene
ΦX174_H_Sanger_fw	GTGGCGCCATGTCTAAATTG	2974-2993	59˚C	56˚C	Sanger sequencing of ΦX174's *H* gene
ΦX174_H_Sanger_fw2	CAGCAAACGCAGAATCAGC	3720-3738	60˚C	56˚C	Sanger sequencing of ΦX174's *H* gene
ΦX174_H_Sanger_rv	CCACAAGCCTCAATAGCAG	4054-4072	58˚C	56˚C	Sanger sequencing of ΦX174's *H* gene
ΦX174_H_Sanger_rv2	CTTTATCAGCGGCAGACTTG	3251-3270	58˚C	56˚C	Sanger sequencing of ΦX174's *H* gene

785

786 **Table S6. List of primers used in this study.** Tm 2Q5: melting temperature of the primer used with the Q5® High-Fidelity 2X Master
787 Mix (NEB). Ta 2Q5: annealing temperature of the set of primers used with the Q5® High-Fidelity 2X Master Mix (NEB). Tm Phusion
788 (buffer HF): melting temperature of the primer used with Phusion® High-Fidelity PCR Master Mix with HF Buffer (ThermoFisher). Ta
789 Phusion (buffer HF): annealing temperature of the primer used with Phusion® High-Fidelity PCR Master Mix with HF Buffer
790 (ThermoFisher).

791 **Supplementary Methods**

792

793 In this section, we provide a more detailed version of the protocols used in the **Methods** section.

794

795 **First phage evolution experiment - Standard**. The protocol from Bono *et al.*[70] was adapted to
796 evolve phages that can infect resistant *E. coli* C strains. Of R1-R35 – the 35 *E. coli* C strains resistant
797 to ΦX174 wildtype, see above – 31 were used for the first phage evolution experiment (excluding R1,
798 R3, R15, and R19; see **Results** and **Text S1**). Thirty-one ΦX174 lineages were each founded by
799 ΦX174 wildtype and serially transferred in cultures containing a mix of *E. coli* C wildtype (permissive
800 strain) and one resistant *E. coli* C strain (non-permissive strain; R2-R35). For each transfer, permissive
801 and non-permissive bacteria were grown separately until they reached log phase. These cultures were
802 founded with an initial inoculum of 180 μl (fast and intermediate growers) or 350 μl (slow growers)
803 of overnight culture (see **Fig. S4**). Fast and intermediate growers were then incubated at 37°C (250
804 rpm) for two hours, slow growers for three hours. Then, permissive and non-permissive strains were
805 mixed in a 14 ml sterile tube at a specific ratio depending on the growth of the non-permissive strain
806 (1:1 for fast growers, 1:2 for intermediate growers, 1:3 for slow growers), to a final volume of 5 ml.
807 At each transfer, ~10^8 freshly prepared susceptible cells were infected by ~10^7 ΦX174 (MOI_{input} ~
808 0.1). Infected cultures were shaken at 250 rpm at 37°C for three hours. Phage lysates were isolated as
809 described in **Phage lysate preparation**. Phage lysates from the previous day were used to inoculate
810 the fresh bacterial mixes the next day. Transfers continued until phages were found to infect their
811 corresponding resistant *E. coli* C strain, or until 21 transfers were reached. Three control lines were
812 also run in parallel, by transferring ΦX174 at MOI_{input} ~ 0.1 in a culture containing *E. coli* C wildtype
813 only.

814

815 **Second phage evolution experiment – Increased diversity.** Four independent ΦX174 lineages
816 were founded by a phage cocktail made of (i) the wildtype ΦX174 and (ii) all isogenic ΦX174 strains
817 that successfully re-infected their corresponding resistant strains during the first phage evolution
818 experiment at a roughly equal number of plaque forming units (final concentration of ~ 2.10^8 pfu/ml).
819 These isogenic phage strains (14 in total) are namely: ΦX174 R4 T7, ΦX174 R5 T2, ΦX174 R8 T6,
820 ΦX174 R10 T6, ΦX174 R13 T6, ΦX174 R18 T4, ΦX174 R19 T1, ΦX174 R20 T5, ΦX174 R21 T1,
821 ΦX174 R24 T1, ΦX174 R26 T1, ΦX174 R27 T1, ΦX174 R29 T1, and ΦX174 R31 T1. Despite being
822 removed from the mutational analysis, phages infecting R5 and R19, respectively, were part of the

823 final cocktail (see **Text S1** and **Table S4**). Each lineage was transferred daily for up to four days, on
824 non-evolving host cultures containing (i) *E. coli* C wildtype, (ii) the 14 host strains for which resistance
825 had been overcome (permissive hosts), and (iii) an excess of the still-resistant strain of interest (non-
826 permissive host). For the non-permissive host, we used R6 (*waaP/pssA* mutant), R22 (*galU* mutant),
827 R25 (*rfaH* mutant), or R28 (*waaG* mutant; see **Table S1**). *E. coli* C R22 and R28 were chosen as
828 representatives of the *galU* and *waaG* mutants, respectively. First, each bacterial strain (permissive and
829 non-permissive) was grown separately in LB liquid culture for one hour (37˚C, 250 rpm). An inoculum
830 of 180 μl from overnight cultures was used for the fast and intermediate growers, while 350 μl was
831 used for the slow growers. After the incubation time, permissive strains were pooled at roughly equal
832 number of colony forming units (CFU), for a final concentration of ~ 10^8 susceptible, permissive cells.
833 One of the *E. coli* C resistant strains of interest was then added in excess (in between ~1 and $5x10^8$
834 resistant cells) in the host mix, to give a final volume of 4 ml. Infections were initiated by adding ~10^7
835 phages (MOI_{input} ~ 0.1) from the phage cocktail to the bacterial culture mix. Infected cultures were
836 shaken in 100 ml sterile Erlenmeyer at 250 rpm, 37˚C, for 5 hours. Phage lysates were isolated as
837 described in **Phage lysate preparation**. Phage lysates from the previous day were used to inoculate
838 the fresh bacterial mixes the next day. This process was repeated until phages were found to infect
839 their corresponding resistant *E. coli* C strains, or until four transfers had been completed.
840
841 **Third evolution experiment – Increased diversity and generations.** Two independent ΦX174
842 lineages were founded by the same phage cocktail used in the second phage evolution experiment.
843 Protocol from the second evolution experiment was adjusted to reduce the amount of time necessary
844 to retrieved the desired phages. We increased the number of lineages' transfers per day from one to
845 four, for a total of four days (16 transfers). *E. coli* C R6 (*waaP/pssA* mutant) and R25 (*rfaH* mutant,
846 see **Table S1**) were used as non-permissive hosts. First, each bacterial strain (permissive and non-
847 permissive) was grown separate for one hour. Then, three bacterial mixes were generated depending
848 on the growth categories of each bacterium (slow, intermediate, and fast growers, **Fig. S4**). 1 ml of
849 each fast grower was used to make the fast mix, 833 μl of each intermediate grower was used for the
850 intermediate mix. Finally, 1.25 ml of each slow grower was used to prepare the slow mix. Bacterial
851 mixes were kept in exponential growth phase independently by transferring every hour 1:5 of the
852 volume (1ml) in fresh LB pre-heated at 37˚C. Before adding the phage cocktail, the three mixes were
853 pooled together (500 μl each, for a total of ~10^8 susceptible cells) and one of the *E. coli* C resistant

854 strains of interest was added in excess (i.e., the number of resistant cells was comprised between ~1
855 and 5.10^8), for a final volume of 4ml. Infections started by adding ~10^7 phages (MOI_{input} ~ 0.1) from
856 the cocktail in the final bacterial mix. Infected cultures were shaken in 100 ml sterile Erlenmeyer at
857 250 rpm, 37°C, for one hour. After that, 1:15 of the volume of each infected culture was transferred
858 in freshly mixed bacterial cultures and infection continued for one hour. This step was repeated for a
859 total of four transfers. The final (fourth) transfer lasted for two hours. All transfers completed on the
860 same day involved transferring both phage and bacteria; on every fourth transfer, supernatants were
861 collected and only phage transferred. Phage lysates were isolated as described in **Phage lysate**
862 **preparation**. Phage lysates from the previous day were used to inoculate the first fresh bacterial mixes
863 the next day.
864
865 **Isolation of evolved ΦX174 strains from evolution experiments.** Top agar overlays were prepared
866 by mixing 100 µl of undiluted phage lysates with 200 µl of overnight culture of the corresponding
867 resistant *E. coli* C strain in 4 ml SSA. Top agar overlays were poured onto LB plates, dried for at least
868 15 minutes, and incubated inverted at 37°C for ~16-17 hours. Plaques were counted the next day. An
869 isolated plaque was chosen randomly for each phage lysate to infect cultures of the corresponding
870 resistant *E. coli* C strains (in exponential growth state) incubated at 37°C, 250 rpm, for 5 hours. Phage
871 lysates were isolated as described in **Phage lysate preparation**. Phage isolates were re-isolated from
872 single plaques a second time from their glycerol stocks. For each phage isolate, a plaque was randomly
873 chosen to infect cultures of the corresponding resistant *E. coli* C strains (in exponential growth state),
874 incubated at 37°C, 250 rpm, for 5 hours. Phage lysates were isolated and stored as described in **Phage**
875 **lysate preparation**.
876
877 **Determination of the evolved phages' host range by spotting assays**
878 *Method 1*. Each top agar overlay was prepared by mixing 200 µl of an *E. coli* C strain from stationary
879 phase culture in 4 ml SSA, then poured on LB plates and dried for at least 15 minutes under a sterile
880 laminar flow hood. Then, 3 µl of each undiluted evolved phage lysate (between 10^7 and 10^9 pfu ml^{-1})
881 was dropped at the surface. *Method 2*. Each top agar overlay was prepared by mixing a volume of each
882 phage lysate in 4 ml SSA at a final concentration of ~10^7 pf ml^{-1}, then poured on LB plates and dried
883 for at least 15 minutes under a sterile laminar flow hood. Then, 3 µl of both undiluted and ten-fold
884 diluted of each *E. coli* C strain (from overnight culture) were dropped onto the surface with a pipette.

885 For both methods, phage lysate spots were dried for at least 30 minutes under sterile laminar flow,
886 and the plates subsequently incubated inverted at 37°C for ~17 hours. *E. coli* C wildtype was used as
887 a positive control (permissive strain), and *E. coli* K-12 MG1655 as a negative control (non-permissive
888 strain). A bacterial host strain was classified as sensitive only when signs of lysis were detected using
889 both methods, in at least two (of three) replicates per method. A phage-bacterium combination that
890 yielded different results between the two methods was tested in standard plaque assays as follows: a
891 top agar overlay was prepared by mixing 100 μl of the phage lysate diluted to 10^{-1} and 10^{-6} with 200
892 μl of the resistant *E. coli* C strain from stationary phase culture in 4 ml SSA, then poured on LB plates
893 and dried for at least 15 minutes. The presence or absence of plaques was assessed the next day.
894 Finally, the host strain was classified as sensitive if plaques was observed at both dilutions.
895
896

897 **References**

898 1. Murray, C. J. *et al.* Global burden of bacterial antimicrobial resistance in 2019: a systematic analysis.
899 *The Lancet* **399**, 629–655 (2022).

900 2. WHO Antimicrobial resistance (2021) at https://www.who.int/news-room/fact-
901 sheets/detail/antimicrobial-resistance.

902 3. Centers for Disease Control and Prevention (U.S.). Antibiotic resistance threats in the United
903 States, 2019 at https://stacks.cdc.gov/view/cdc/82532.

904 4. Bull, J. J., Levin, B. R. & Molineux, I. J. Promises and pitfalls of *in vivo* evolution to improve phage
905 therapy. *Viruses* **11**, 1083 (2019).

906 5. Oechslin, F. Resistance development to bacteriophages occurring during bacteriophage therapy.
907 *Viruses* **10**, 351 (2018).

908 6. Monteiro, R., Pires, D. P., Costa, A. R. & Azeredo, J. Phage therapy: going temperate? *Trends*
909 *Microbiol.* **27**, 368–378 (2019).

910 7. Zhang, G., Meredith, T. C. & Kahne, D. On the essentiality of lipopolysaccharide to Gram-
911 negative bacteria. *Curr. Opin. Microbiol.* **16**, 779–785 (2013).

912 8. Nikaido, H. Molecular basis of bacterial outer membrane permeability revisited. *Microbiol. Mol.*
913 *Biol. Rev.* **67**, 593–656 (2003).

914 9. Mutalik, V. K. *et al.* High-throughput mapping of the phage resistance landscape in *E. coli*. *PLOS*
915 *Biol.* **18**, e3000877 (2020).

916 10. Simpson, B. W. & Trent, M. S. Pushing the envelope: LPS modifications and their consequences.
917 *Nat. Rev. Microbiol.* **17**, 403–416 (2019).

918 11. Schnaitman, C. A. & Klena, J. D. Genetics of lipopolysaccharide biosynthesis in enteric bacteria.
919 *Microbiol. Rev.* **57**, 655–682 (1993).

920 12. Raetz, C. R. H. & Whitfield, C. Lipopolysaccharide endotoxins. *Annu. Rev. Biochem.* **71**, 635–700
921 (2002).

922 13. Qian, J., Garrett, T. A. & Raetz, C. R. H. *In vitro* assembly of the outer core of the
923 lipopolysaccharide from *Escherichia coli* K-12 and *Salmonella typhimurium*. *Biochemistry* **53**, 1250–1262
924 (2014).

925 14. Klein, G. & Raina, S. Regulated assembly of LPS, its structural alterations and cellular response
926 to LPS defects. *Int. J. Mol. Sci.* **20**, 356 (2019).

927 15. Amor, K. *et al.* Distribution of core oligosaccharide types in lipopolysaccharides from *Escherichia*
928 *coli*. *Infect. Immun.* **68**, 1116–1124 (2000).

929 16. Klein, G. *et al.* Molecular and structural basis of inner core lipopolysaccharide alterations in
930 *Escherichia coli*: incorporation of glucuronic acid and phosphoethanolamine in the heptose region.
931 *J. Biol. Chem.* **288**, 8111–8127 (2013)

932 17. Yethon, J. A., Heinrichs, D. E., Monteiro, M. A., Perry, M. B. & Whitfield, C. Involvement of
933 *waaY*, *waaQ*, and *waaP* in the modification of *Escherichia coli* lipopolysaccharide and their role in the
934 formation of a stable outer membrane. *J. Biol. Chem.* **273**, 26310–26316 (1998).

935 18. Whitfield, C. *et al.* Assembly of the R1-type core oligosaccharide of *Escherichia coli*
936 lipopolysaccharide. **5**, 151–156 (1999).

937 19. Van der Ley, P., de Graaff, P. & Tommassen, J. Shielding of *Escherichia coli* outer membrane
938 proteins as receptors for bacteriophages and colicins by O-antigenic chains of lipopolysaccharide.
939 *J. Bacteriol.* **168**, 449–451 (1986).

940 20. Pagnout, C. *et al.* Pleiotropic effects of *rfa*-gene mutations on *Escherichia coli* envelope properties.
941 *Sci. Rep.* **9**, 9696 (2019).

942 21. Matsuura, M. Structural modifications of bacterial lipopolysaccharide that facilitate Gram-negative
943 bacteria evasion of host innate immunity. *Front. Immunol.* **4**, (2013).

944 22. Hancock, R. E. & Reeves, P. Lipopolysaccharide-deficient, bacteriophage-resistant mutants of
945 *Escherichia coli* K-12. *J. Bacteriol.* **127**, 98–108 (1976).

946 23. Labrie, S. J., Samson, J. E. & Moineau, S. Bacteriophage resistance mechanisms. *Nat. Rev. Microbiol.*
947 **8**, 317–327 (2010).

948 24. Kulikov, E. E., Golomidova, A. K., Prokhorov, N. S., Ivanov, P. A. & Letarov, A. V. High-
949 throughput LPS profiling as a tool for revealing of bacteriophage infection strategies. *Sci. Rep.* **9**,
950 2958 (2019).

951 25. Sanger, F *et al.* The nucleotide sequence of Bacteriophage ΦX174. *J. Mol. Biol.* **125**, 225–246 (1978).

952 26. Sinsheimer, R. L. A single-stranded deoxyribonucleic acid from bacteriophage ΦX174. *J. Mol. Biol.*
953 **1**, 43–53 (1959).

954 27. Incardona, N. L. & Selvidge, L. Mechanism of adsorption and eclipse of bacteriophage ΦX174
955 II. Attachment and eclipse with isolated *Escherichia coli* cell wall lipopolysaccharide. *J. Virol.* **11**,
956 775–782 (1973).

957 28. Incardona, N. L., Tuech, J. K. & Murti, G. Irreversible binding of phage ΦX174 to cell-bound
958 lipopolysaccharide receptors and release of virus-receptor complexes. *Biochemistry* **24**, 6439–6446
959 (1985).

960 29. Sun, Y. *et al.* Structural changes of tailless bacteriophage ΦX174 during penetration of bacterial
961 cell walls. *Proc. Natl. Acad. Sci.* **114**, 13708–13713 (2017).

962 30. Michel, A., Clermont, O., Denamur, E. & Tenaillon, O. Bacteriophage ΦX174's Ecological niche
963 and the flexibility of its *Escherichia coli* lipopolysaccharide receptor. *Appl. Environ. Microbiol.* **76**,
964 7310–7313 (2010).

965 31. Feige, Ulrich & Stirm, Stephan. On the structure of *Escherichia coli* C cell wall lipopolysaccharide
966 core and its ΦX174 receptor region. *Biochem. Biophys. Res. Commun.* **71**, 8 (1976).

967 32. Inagaki, M. *et al.* Characterization of the binding of spike H protein of bacteriophage ΦX174 with
968 receptor lipopolysaccharides. *J. Biochem. (Tokyo)* **127**, 577–583 (2000).

969 33. Kawaura, T. *et al.* Recognition of receptor lipopolysaccharides by spike G protein of bacteriophage
970 ΦX174. *Biosci. Biotechnol. Biochem.* **64**, 1993–1997 (2000).

971 34. Król, J. E. *et al.* Genome rearrangements induce biofilm formation in *Escherichia coli* C – an old
972 model organism with a new application in biofilm research. *BMC Genomics* **20**, 767 (2019).

973 35. Kojima, H., Inagaki, M., Tomita, T. & Watanabe, T. Diversity of non-stoichiometric substitutions
974 on the lipopolysaccharide of *E. coli* C demonstrated by electrospray ionization single quadrupole
975 mass spectrometry. *Rapid Commun. Mass Spectrom.* **24**, 43–48 (2010).

976 36. Luria, S. E. & Delbrück, M. Mutations of bacteria from virus sensitivity to virus resistance. *Genetics*
977 **28**, 491–511 (1943).

978 37. Lind, P. A., Libby, E., Herzog, J. & Rainey, P. B. Predicting mutational routes to new adaptive
979 phenotypes. *eLife* **8**, e38822 (2019).

980 38. Moxon, E. R., Rainey, P. B., Nowak, M. A. & Lenski, R. E. Adaptive evolution of highly mutable
981 loci in pathogenic bacteria. *Curr. Biol.* **4**, 24–33 (1994).

982 39. Yethon, J. A., Vinogradov, E., Perry, M. B. & Whitfield, C. Mutation of the lipopolysaccharide
983 core glycosyltransferase encoded by *waaG* destabilizes the outer membrane of *Escherichia coli* by
984 interfering with core phosphorylation. *J. Bacteriol.* **182**, 5620–5623 (2000).

985 40. Bailey, M. J. A., Hughes, C. & Koronakis, V. RfaH and the *ops* element, components of a novel
986 system controlling bacterial transcription elongation. *Mol. Microbiol.* **26**, 845–851 (1997).

987 41. Hermisson, J. & Pennings, P. S. Soft sweeps: molecular population genetics of adaptation from
988 standing genetic variation. *Genetics* **169**, 2335–2352 (2005).

989 42. Barrett, R. D. H. & Schluter, D. Adaptation from standing genetic variation. *Trends Ecol. Evol.* **23**,
990 38–44 (2008).

991 43. Sant, D. G., Woods, L. C., Barr, J. J. & McDonald, M. J. Host diversity slows bacteriophage
992 adaptation by selecting generalists over specialists. *Nat. Ecol. Evol.* **5**, 350–359 (2021).

993 44. Rokyta, D. R., Burch, C. L., Caudle, S. B. & Wichman, H. A. Horizontal gene transfer and the
994 evolution of microvirid coliphage genomes. *J. Bacteriol.* **188**, 1134–1142 (2006).

995 45. Betts, A., Gray, C., Zelek, M., MacLean, R. C. & King, K. C. High parasite diversity accelerates
996 host adaptation and diversification. *Science* **360**, 907–911 (2018).

997 46. McKenna, R. *et al.* Atomic structure of single-stranded DNA bacteriophage ΦX174 and its
998 functional implications. *Nature* **355**, 137–143 (1992).

999 47. Cox, J. & Putonti, C. Mechanisms responsible for a ΦX174 mutant's ability to Infect *Escherichia*
1000 *coli* by phosphorylation. *J. Virol.* **84**, 4860–4863 (2010).

1001 48. Crill, W. D., Wichman, H. A. & Bull, J. J. Evolutionary reversals during viral adaptation to
1002 alternating hosts. *Genetics* **154**, 27–37 (2000).

1003 49. Weisbeek, P. J., Van de Pol, J. H. & Van Arkel, G. A. Mapping of host range mutants of
1004 bacteriophage ΦX174. *Virology* **52**, 408–416 (1973).

1005 50. Bull, J. J. *et al.* Exceptional convergent evolution in a virus. *Genetics* **147**, 1497–1507 (1997).

1006 51. Wichman, H. A., Badgett, M. R., Scott, L. A., Boulianne, C. M. & Bull, J. J. Different trajectories
1007 of parallel evolution during viral adaptation. *Science* **285**, 422–424 (1999).

1008 52. Remold, S. K., Rambaut, A. & Turner, P. E. Evolutionary genomics of host adaptation in vesicular
1009 stomatitis virus. *Mol. Biol. Evol.* **25**, 1138–1147 (2008).

1010 53. Bertels, F., Leemann, C., Metzner, K. J. & Regoes, R. R. Parallel evolution of HIV-1 in a long-
1011 term experiment. *Mol. Biol. Evol.* **36**, 2400–2414 (2019).

1012 54. Bertels, F., Metzner, K. J. & Regoes, R. Convergent evolution as an indicator for selection during
1013 acute HIV-1 infection. *Peer Community J.* **1**, e4 (2021).

1014 55. Kneidinger, B. *et al.* Biosynthesis Pathway of ADP-L-glycero-ᴺ-D-manno-Heptose in *Escherichia*
1015 *coli*. *J. Bacteriol.* **184**, 7 (2002).

1016 56. Bertozzi Silva, J., Storms, Z. & Sauvageau, D. Host receptors for bacteriophage adsorption. *FEMS*
1017 *Microbiol. Lett.* **363**, fnw002 (2016).

1018 57. Latino, L., Midoux, C., Hauck, Y., Vergnaud, G. & Pourcel, C. Pseudolysogeny and sequential
1019 mutations build multiresistance to virulent bacteriophages in *Pseudomonas aeruginosa*. *Microbiol. Read.*
1020 *Engl.* **162**, 748–763 (2016).

1021 58. Broeker, N. K. & Barbirz, S. Not a barrier but a key: how bacteriophages exploit host's O-antigen
1022 as an essential receptor to initiate infection. *Mol. Microbiol.* **105**, 353–357 (2017).

1023 59. Meyer, J. R. *et al.* Repeatability and contingency in the evolution of a key innovation in phage
1024 Lambda. *Science* **335**, 428–432 (2012).

1025 60. Burmeister, A. R., Lenski, R. E. & Meyer, J. R. Host coevolution alters the adaptive landscape of
1026 a virus. *Proc. R. Soc. B Biol. Sci.* **283**, 20161528 (2016).

1027 61. Gupta, A. *et al.* Host-parasite coevolution promotes innovation through deformations in fitness
1028 landscapes. *eLife* **11**, e76162 (2022).

1029 62. Bearden, C. M. *et al.* Rituximab inhibits the *in vivo* primary and secondary antibody response to a
1030 neoantigen, bacteriophage ΦX174. *Am. J. Transplant. Off. J. Am. Soc. Transplant. Am. Soc. Transpl.*
1031 *Surg.* **5**, 50–57 (2005).

1032 63. Rubinstein, A. *et al.* Progressive specific immune attrition after primary, secondary and tertiary
1033 immunizations with bacteriophage ΦX174 in asymptomatic HIV-1 infected patients. *AIDS Lond.*
1034 *Engl.* **14**, F55-62 (2000).

1035 64. Chan, B. K. *et al.* Phage treatment of an aortic graft infected with *Pseudomonas aeruginosa*. *Evol. Med.*
1036 *Public Health* **2018**, 60–66 (2018).

1037 65. Krüger, A. & Lucchesi, P. M. A. Shiga toxins and stx phages: highly diverse entities. *Microbiol.*
1038 *Read. Engl.* **161**, 451–462 (2015).

1039 66. Jamet, A. *et al.* A widespread family of polymorphic toxins encoded by temperate phages. *BMC*
1040 *Biol.* **15**, 75 (2017).

1041 67. Ramjeet, M. *et al.* Truncation of the lipopolysaccharide outer core affects susceptibility to
1042 antimicrobial peptides and virulence of *Actinobacillus pleuropneumoniae* serotype 1. *J. Biol. Chem.* **280**,
1043 39104–39114 (2005).

1044 68. Maldonado, R. F., Sá-Correia, I. & Valvano, M. A. Lipopolysaccharide modification in Gram-
1045 negative bacteria during chronic infection. *FEMS Microbiol. Rev.* **40**, 480–493 (2016).

1046 69. Burmeister, A. R. *et al.* Pleiotropy complicates a trade-off between phage resistance and antibiotic
1047 resistance. *Proc. Natl. Acad. Sci.* **117**, 11207–11216 (2020).

1048 70. Bono, L. M., Gensel, C. L., Pfennig, D. W. & Burch, C. L. Competition and the origins of novelty:
1049 experimental evolution of niche-width expansion in a virus. *Biol. Lett.* **9**, 20120616–20120616
1050 (2012).

1051 71. Picelli, S. *et al.* Tn5 transposase and tagmentation procedures for massively scaled sequencing
1052 projects. *Genome Res.* **24**, 2033–2040 (2014).

1053 72. Deatherage, D. E. & Barrick, J. E. Identification of mutations in laboratory-evolved microbes
1054 from next-generation sequencing data using *breseq*. *Methods Mol. Biol. Clifton NJ* **1151**, 165–188
1055 (2014).

1056 73. Barrick, J. E. *et al.* Identifying structural variation in haploid microbial genomes from short-read
1057 resequencing data using *breseq*. *BMC Genomics* **15**, 1039 (2014).

1058 74. Deatherage, D. E., Traverse, C. C., Wolf, L. N. & Barrick, J. E. Detecting rare structural variation
1059 in evolving microbial populations from new sequence junctions using *breseq*. *Front. Genet.* **5**, (2015).

1060 75. Fang, J. & Wei, Y. Expression, purification and characterization of the *Escherichia coli* integral
1061 membrane protein YajC. *Protein Pept. Lett.* **18**, 601–608 (2011).

1062 76. Schulze, R. J. *et al.* Membrane protein insertion and proton-motive-force-dependent secretion
1063 through the bacterial holo-translocon SecYEG–SecDF–YajC–YidC. *Proc. Natl. Acad. Sci.* **111**,
1064 4844–4849 (2014).

1065 77. Bohm, K. *et al.* Genes affecting progression of bacteriophage P22 infection in *Salmonella* identified
1066 by transposon and single gene deletion screens: host genes affecting phage P22 infection. *Mol.*
1067 *Microbiol.* **108**, 288–305 (2018).

1068 78. Belunis, C. J., Clementz, T., Carty, S. M. & Raetz, C. R. H. Inhibition of lipopolysaccharide
1069 biosynthesis and cell growth following inactivation of the *kdtA* gene in *Escherichia coli*. *J. Biol. Chem.*
1070 **270**, 27646–27652 (1995).

1071 79. Klein, G., Lindner, B., Brabetz, W., Brade, H. & Raina, S. *Escherichia coli* K-12 suppressor-free
1072 mutants lacking early glycosyltransferases and late acyltransferases: Minimal lipopolysaccharide
1073 structure and induction of envelope stress response. *J. Biol. Chem.* **284**, 15369–15389 (2009).

1074 80. Jansson, P.-E., Lindberg, B., Lindberg, A. A. & Wollin, R. Structural studies on the hexose region
1075 of the core in lipopolysaccharides from Enterobacteriaceae. *Eur. J. Biochem.* **115**, 571–577 (1981).

1076 81. Heinrichs, D. E., Yethon, J. A. & Whitfield, C. Molecular basis for structural diversity in the core
1077 regions of the lipopolysaccharides of *Escherichia coli* and *Salmonella enterica*. *Mol. Microbiol.* **30**, 221–
1078 232 (1998).

1079 82. Vinogradov, E. V. *et al.* The structures of the carbohydrate backbones of the lipopolysaccharides
1080 from *Escherichia coli* rough mutants F470 (R1 core type) and F576 (R2 core type): LPS from *E. coli*
1081 R1 and R2 core types. *Eur. J. Biochem.* **261**, 629–639 (1999).

1082 83. Heinrichs, D. E., Yethon, J. A., Amor, P. A. & Whitfield, C. The assembly system for the outer
1083 core portion of R1- and R4-type lipopolysaccharides of *Escherichia coli*: the R1 core-specific β-
1084 glucosyltransferase provides a novel attachment site for O-polysaccharides. *J. Biol. Chem.* **273**,
1085 29497–29505 (1998).

1086 84. Leipold, M. D., Vinogradov, E. & Whitfield, C. Glycosyltransferases involved in biosynthesis of
1087 the outer core region of *Escherichia coli* lipopolysaccharides exhibit broader substrate specificities
1088 than is predicted from lipopolysaccharide structures. *J. Biol. Chem.* **282**, 26786–26792 (2007).

1089 85. Frey, P. A. The Leloir pathway: a mechanistic imperative for three enzymes to change the
1090 stereochemical configuration of a single carbon in galactose. *FASEB J.* **10**, 461–470 (1996).

1091 86. McArthur, F., Andersson, C. E., Loutet, S., Mowbray, S. L. & Valvano, M. A. Functional analysis
1092 of the glycero-manno-heptose 7-phosphate kinase domain from the bifunctional HldE protein,
1093 which is involved in ADP-L-glycero-D-manno-Heptose biosynthesis. *J. Bacteriol.* **187**, 5292–5300
1094 (2005).

1095 87. Weissborn, A. C., Liu, Q., Rumley, M. K. & Kennedy, E. P. UTP: α-D-glucose-L-phosphate
1096 uridylyltransferase of *Escherichia coli*: isolation and DNA sequence of the *galU* gene and purification
1097 of the enzyme. **176**, 8 (1994).

1098 88. Genevaux, P., Bauda, P., DuBow, M. S. & Oudega, B. Identification of Tn 10 insertions in the
1099 *rfaG*, *rfaP*, and *galU* genes involved in lipopolysaccharide core biosynthesis that affect *Escherichia*
1100 *coli* adhesion. *Arch. Microbiol.* **172**, 1–8 (1999).

1101 89. Pierson, D. E. & Carlson, S. Identification of the *galE* gene and a *galE* homolog and
1102 characterization of their roles in the biosynthesis of lipopolysaccharide in a serotype O:8 strain of
1103 *Yersinia enterocolitica*. *J. Bacteriol.* **178**, 5916–5924 (1996).

1104 90. Schnaitman, C. A. & Austin, E. A. Efficient incorporation of galactose into lipopolysaccharide by
1105 *Escherichia coli* K-12 strains with polar *galE* mutations. *J. Bacteriol.* **172**, 5511–5513 (1990).

1106 91. Karp, P. D. *et al.* The BioCyc collection of microbial genomes and metabolic pathways. *Brief.*
1107 *Bioinform.* **20**, 1085–1093 (2019).

1108

1109

1110 **Contributions**

1111

1112 J.R.D and F.B conceived the study and planned the experiments. J.R.D and L.P. carried out the
1113 experiments. J.R.D conducted the sequence analyses. J.R.D, F.B, and J.G interpreted the results.
1114 J.R.D., F.B., and J.G. wrote the manuscript. J.R.D prepared all figures and tables. All authors reviewed
1115 and approved the manuscript.

1116

1117 **Competing interests**

1118

1119 The authors declare no competing interests.

1120

1121 **Acknowledgments**

1122

1123 We thank Loukas Theodosiou for his bioinformatic support, David Rogers for troubleshooting all
1124 PCRs, and Sven Kuenzel for his help with phage and bacterial genome sequencing.

1125